PENSOFT

SENCKENBERG
world of biodiversity

Leibniz Association

Systematic revision of the *Calotes jerdoni* complex (Reptilia: Squamata: Agamidae) in the Pan-Himalaya

Kai Wang[1,2], V. Deepak[3,4], Abhijit Das[5], L. Lee Grismer[6,7,8], Shuo Liu[9], Jing Che[1,2]

1 *State Key Laboratory of Genetic Resources and Evolution and Yunnan Key Laboratory of Biodiversity and Ecological Conservation of Gaoligong Mountain, Kunming Institute of Zoology, Chinese Academy of Sciences, Kunming, Yunnan, 650223, China*

2 *Southeast Asia Biodiversity Research Institute, Chinese Academy of Sciences, Yezin, Nay Pyi Taw, 05282, Myanmar*

3 *Senckenberg Dresden, Königsbrücker Landstraße 159, 01109 Dresden, Germany*

4 *Science Group, The Natural History Museum, London SW7 5BD, UK*

5 *Wildlife Institute of India, Chandrabani, Dehradun, 248002, India*

6 *Herpetology Laboratory, Department of Biology, La Sierra University, 4500 Riverwalk Parkway, Riverside, California, 92515, USA*

7 *Department of Herpetology, San Diego Natural History Museum, PO Box 121390, San Diego, California, 92112, USA*

8 *Institute for Tropical Biology and Conservation, Universiti Malaysia Sabah, Kota Kinabalu, Malaysia*

9 *Kunming Zoological Museum, Kunming Institute of Zoology, Chinese Academy of Sciences, Kunming, Yunnan, 650223, China*

http://zoobank.org/D85DA495-4568-48EC-B0AA-2A9B48F817EA

Corresponding authors: Kai Wang (wangkai@mail.kiz.ac.cn), Jing Che (chej@mail.kiz.ac.cn)

Academic editors Uwe Fritz | **Received** 5 July 2023 | **Accepted** 13 December 2023 | **Published** 7 March 2024

Citation: Wang K, Deepak V, Das A, Grismer LL, Liu S, Che J (2024) Systematic revision of the *Calotes jerdoni* complex (Reptilia: Squamata: Agamidae) in the Pan-Himalaya. Vertebrate Zoology 74 169–192. https://doi.org/10.3897/vz.74.e109088

Abstract

Owing to the harsh terrain, few biodiversity surveys have been carried out in the Pan-Himalaya Region. Among the understudied taxa from this region, Jerdon's forest lizard, *Calotes jerdoni*, is believed to have a wide distribution, from northeast India to southwestern China. However, given the heterogeneous environment across its range and the lack of studies on this species, its taxonomy remains questionable. Using integrative taxonomic methods, we combined both morphological and genetic data from the type and topotypic specimens and examined the current taxonomic hypothesis of *C. jerdoni* across its range. Molecular data reveal that *C. jerdoni* as currently recognized, contains three deeply diverged lineages: one from the type locality in Northeast India, one from Western Myanmar, and another one from Southwestern China. The uncorrected genetic distances of mitochondrial coding gene ND2 among these three clades ranged over 10%. The Chinese population is sister to *C. medogensis* and paraphyletic to the remaining two clades of *C. jerdoni*. Morphological analyses confirm the results of the molecular analyses, where the Myanmar and Chinese populations can be diagnosed statistically in both univariate and multivariate space from the true *C. jerdoni*, as well as by a suite of reliable categorical morphological characters, including the size and shape of gular scales and ventral scales. To resolve the current taxonomic confusion, we resurrect the junior synonym, *C. yunnanensis*, for the Chinese population and expand its distribution to Myanmar, redescribe the elusive *C. maria* and *C. medogensis* based on its type material, and describe the remaining western Myanmar population as a new species. We further discuss the possibility of additional cryptic species within the complex in the Pan-Himalaya Region and provide a diagnostic key to all recognized members of the *C. jerdoni* complex.

Keywords

Dragon lizards, East Himalaya, questionable records, taxonomic revision, Tibet, Xizang Autonomous Region

Introduction

Forest lizards of the genus *Calotes* Cuvier, 1817 represent the third-most diverse Draconinae genus, with a total of 25 currently recognized species (Pal et al. 2018; Uetz et al. 2023). Members of the genus are widely distributed throughout Asia, from Sri Lanka across southern Himalaya to Southeast Asia (Manthey 2010). While considerable progress has been made on the taxonomy of the genus in the Indian subcontinent (Deepak et al. 2015; Gowande et al. 2016, 2021; Pal et al. 2018; Giri et al. 2019) and the Indochinese region (Hallermann 2000; Zug et al. 2006; Vindum et al. 2003; Hartmann et al. 2013), far less attention has been given to species from the Pan-Himalayan Region, particularly species of the *C. jerdoni* complex.

First described based on a collection of specimens from the Khassia Hills (= Khasi Hills) in northeast India, *C. jerdoni* Günther, 1870 was diagnosed from *C. maria* Gray, 1845 by having a shorter distance between the supratympanic spikes and the tympanum, larger gular scales, and shorter and more compact nuchal crest scales (Günther 1870). Thirty-five years later, Annandale (1905) described another species, *C. yunnanensis* Annandale, 1905, from Tengyue County in southwestern Yunnan Province, China. Although *C. yunnanensis* resembles *C. jerdoni* morphologically, it was not compared against *C. jerdoni* in its original description. Smith (1935) first synonymized *C. yunnanensis* with *C. jerdoni* without any explicit explanation, and this taxonomic hypothesis went unquestioned by all subsequent workers (Zhao and Adler 1993; Zhao and Yang 1997; Zhao et al. 1999; Yang and Rao 2008; Manthey 2010; Pal et al. 2018; Wang et al. 2020, 2022). In addition to the recently reported records of *C. jerdoni* from western Myanmar (Zug et al. 2006), *C. jerdoni* has now become a widespread species ranging from the East Himalaya to northern Indochina, and across northeast India, Myanmar, and China (Smith 1935; Zhao et al. 1999; Yang and Rao 2008; Tshewang and Letro 2018).

Che et al. (2020) showed that the Chinese population of *C.* cf. *jerdoni* (identified as *Calotes* sp. in Che et al. 2020, from the type locality of its junior synonym *C. yunnanensis*, is paraphyletic with respect to the Myanmar population of *C. jerdoni*. This result raised questions on the previous synonymy between *C. yunnanensis* and *C. jerdoni* by Smith (1935). Similar results were shown by Boruah et al. (2022), where the Chinese population of *C.* cf. *jerdoni* is paraphyletic with respect to both western Myanmar and Indian populations of *C. jerdoni*. Moreover, because the currently recognized populations of *C.* cf. *jerdoni* from southwestern China and western Myanmar are both allopatric with respect to true *C. jerdoni*, separated by the Chin Hills and Central Dry Zone of Myanmar—geographic features known to be barriers for agamids (e.g., *Ptyctolaemus*, Schulte et al. 2004 and the *Calotes versicolor* group, Vindum et al. 2003), — and given that the western Myanmar population showed considerable genetic divergences with respect to Indian topotypic population (Boruah et al. 2022), it is likely that *C. jerdoni* as currently known, also contains cryptic lineages, and the validity of *C. yunnanensis* warrants further examination. Unfortunately, no detailed morphological data of either the type or topotypic specimens of *C. yunnanensis* have ever been reported, particularly regarding useful scale counts used in recent taxonomic studies.

In relation to *C. jerdoni*, the taxonomy of other recognized species of the complex, namely *C. maria* and *C. medogensis* Zhao & Li, 1984, is also unsettled. *Calotes maria* was first described based on four syntypes from Afghanistan and Khassia Hill (Gray 1845), but later Boulenger (1885) identified three of the four syntypes of *C. maria* as *C. jerdoni*, and he selected NHMUK 1946.8.1.24 as the "type" of *C. maria.* This action constitutes a lectotype designation in accordance with Article 74.5 of the International Code of Zoological Nomenclature (ICZN 1999). To date, the species is known from the lectotype only, and little is known about the species morphology other than from its original description. On the other hand, *C. medogensis* was first described based on a single specimen from southeastern Xizang Autonomous Region (= Tibet), China, and it was compared to *C. nemoricola* Jerdon, 1853 only (Zhao and Li 1984), despite its obvious resemblances to the *C. jerdoni* complex. Subsequent authors all considered *C. medogensis* as a valid species without providing any additional comparisons to members of the *C. jerdoni* complex (Zhao et al. 1999; Li et al. 2010; Ananjeva et al. 2011; Wang et al. 2020). It was not until Che et al. (2020) provided the first expanded description of *C. medogensis* based on additional specimens that it was done. Nevertheless, Che et al. (2020) only reported a few morphological characters from the examined specimens. While stating that *C. medogensis* resembled *C. maria*, however, the morphological comparison by Che et al. (2020) was based on data from the literature on *C. maria*, which are quite abstract. Recently, Boruah et al. (2022) designated a lectotype for *C. jerdoni* and reported additional specimens of *C. medogensis*. While they compared *C. jerdoni* with *C. medogensis*, such a comparison was not based on the type or topotypic specimens of *C. medogensis*. Without examining the relevant type material of *C. maria* and *C. medogensis*, it remains difficult to obtain a comprehensive understanding of the *C. jerdoni* complex and to statistically diagnose species with confidence.

Fortunately, international collaborations allow a broader genetic and morphological sampling across the range of *C. jerdoni* complex, including access to the type series and topotypic materials. Combining both mitochondrial DNA and morphological data, we examine the current taxonomic hypotheses within the *C. jerdoni* complex from the Pan-Himalaya Region, particularly regarding the validity of its junior synonym, *C. yunnanensis*, the validity of *C. medogensis* with respect to *C. maria*, and the taxonomic identity of the western and northern Myanmar population of *C.* cf. *jerdoni.*

Materials and methods

Sampling

Voucher specimens were examined from museum collections, including type specimens of *C. jerdoni*, *C. maria*, *C. medogensis*, and *C. yunnanensis*; topotypes of *C. jerdoni*, *C. medogensis* and *C. yunnanensis*; and specimens of *C.* cf. *jerdoni* from Chin and Kachin States of Myanmar (Fig. 1; Appendix I). Museum abbreviations are the following: California Academy of Sciences (**CAS**), Chengdu Institute of Biology, Chinese Academy of Sciences (**CIB**), Kunming Institute of Zoology, Chinese Academy of Sciences (**KIZ**), Zoological Survey of India (**ZSI**), and the Natural History Museum, London (**NHMUK**).

Phylogenetic analyses

The coding region of the mitochondrial gene ND2 from 14 species of *Calotes* and representatives of other Draconinae genera were obtained from GenBank (Table 1). Outgroup taxa (*Salea*, *Bronchocela*, and *Pseudocalotes*) were chosen based on Wang et al. (2019a; Table 1). All sequences were edited and aligned using MUSCLE in Geneious Prime v2022.2.1. The final alignment contained 1026 bp with a sample size of 27 individuals.

Bayesian inference and Maximum Likelihood analyses were conducted on the final alignment. Bayesian analysis was done using the program MrBayes v. 3.2.7a (Ronquist et al. 2012) on CIPRES. The ND2 coding region was partitioned by codon. Using JMODELTEST2 v. 2.1.10 (Guindon and Gascuel 2003; Darriba et al. 2012), the best evolutionary model of nucleotide substitution was selected for each codon postion, which inferred the model GTR + Γ for all. Two independent Markov Chain Monte Carlo analyses were run, each with four Metropolis-coupled chains, a melting temperature of 0.02, and an exponential distribution with a rate parameter of 25 as the prior on branch lengths (Marshall 2010). Each run was conducted with 100 million generations and sampled every 2,000 generations, discarding the first 20% of trees as burn-in. Convergence of runs was confirmed with TRACER v. 1.7.0 (visual convergence and Effective Sampling Size>200; Rambaut et al. 2018).

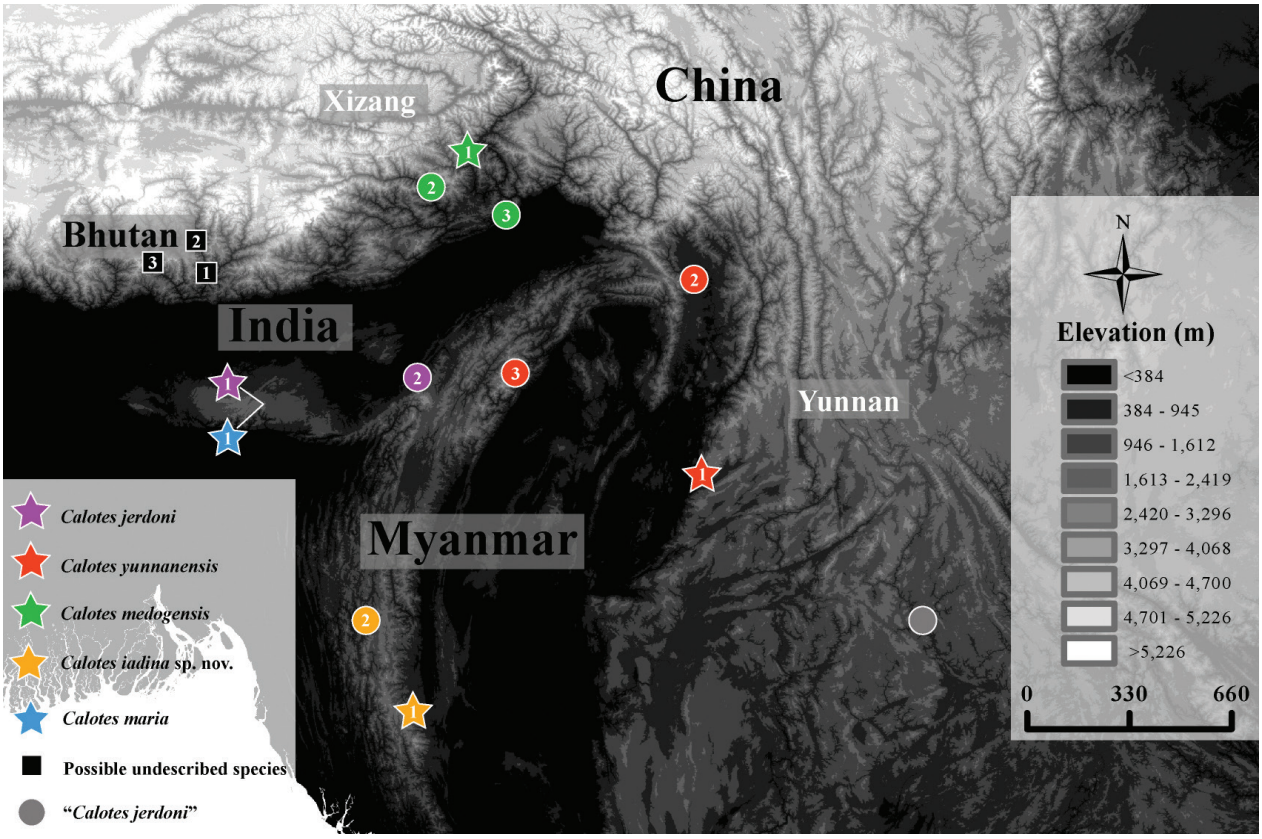

Figure 1. Distribution of *Calotes jerdoni* complex in the Pan-Himalaya Region. Localities are based of vouchered specimens (Appendix I) and literature (Zhao et al. 1999; Yang and Rao 2008; Tshewang and Letro 2018; Lwin et al. 2021; Boruah et al. 2022). Stars indicate type localities, circles represent additional localities of a given species, and rectangles represent localities of potential cryptic species. Different colors represent different species, which include *C. jerdoni* (purple): (**1**) Khasi Hills, Meghalaya, India, (**2**) Kohima District, Nagaland, India; *C. medogensis* (green): (**1**) Medog, Nynchi Prefecture, Xizang Autonomous Region, China; (**2**) and (**3**): East Himalaya (see Boruah et al. 2022 for details); *C. iadina* **sp. nov.** (yellow): (**1**) Nat Ma Taung National Park, Min Dat District, Chin State, Myanmar; (**2**) Phalum Township, Phalum District, Chin State, Myanmar; *C. yunnanensis* (red): (**1**) Yingjiang County, Yunnan Province, China, (**2**) Putao District, Myanmar; and (**3**) Khandi District, Sagaing Division, Myanmar; and possible undescribed species (black). Possible undescribed species are presented, including: Mongar (**1**), Lhuentse (**2**), and Langthel (**3**) in Bhutan.

Table 1. GenBank information of samples used.

GenBank Accession Number	Species	Voucher	Locality
OP882616	*Calotes jerdoni*	WII-ADR 999	East Khasi Hill, Meghalaya, India
OP882617	*Calotes jerdoni*	WII-ADR 966	Dzuleke, Nagaland, India
GQ502783	*Calotes iadina* **sp. nov.**	CAS 219992	Chin State, Myanmar
OP882619	*Calotes medogensis*	WII-ADR 1211	East Himalaya
OP882618	*Calotes medogensis*	WII-ADR 452	East Himalaya
MW133376	*Calotes medogensis*	KIZ 07372	Medog, Xizang Autonomous Region, China
MW111455	*Calotes medogensis*	KIZ 013861	Medog, Xizang Autonomous Region, China
MW183285	*Calotes yunnanensis*	KIZ 014146	Yingjiang, Yunnan, China
MW183286	*Calotes yunnanensis*	KIZ 014147	Yingjiang, Yunnan, China
MW183287	*Calotes yunnanensis*	KIZ 014148	Yingjiang, Yunnan, China
GQ502784	*Pseudocalotes kakhienensis*	CAS 207492	Baoshan, Yunnan, China
AF288229	*Bronchocela cristatella*	THNC 56517	Sarawak, Malaysia
KR053124	*Bronchocela shenlong*	LSUHC 9017	Bukit Larut, Malaysia
AF128490	*Salea horsfieldii*	BNHS-AMB5739	Tamil Nadu, India
AF128487	*Calotes mystaceus*	MVZ 222144	Buon Ma Thuot, Vietnam
KT952397	*Calotes minor*	CESG 162	Gujarat, India
DQ289460	*Calotes* cf. *emma*	CAS 223062	Rakhine State, Myanmar
DQ289458	*Calotes chincollium*	CAS 220582	Chin State, Myanmar
DQ289459	*Calotes chincollium*	CAS 215505	Chin State, Myanmar
AF128484	*Calotes liocephalus*	WHT 1632	Knuckles, Sri Lanka
AF128486	*Calotes nigrilabris*	WHT 1680	Sita Eliya, Sri Lanka
AF128483	*Calotes ceylonensis*	WHT 1624	Yodaganawa, Sri Lanka
DQ289461	*Calotes htunwini*	USNM 524044	Sagaing Division, Myanmar
AF128482	*Calotes calotes*	WHT 1679	Navinna, Sri Lanka
AB183287	*Calotes* cf. *versicolor*	NUM AZ382	Unknown
DQ289478	*Calotes* cf. *versicolor*	CAS 208157	Yangon Division, Myanmar
DQ289468	*Calotes irawadi*	CAS 204862	Sagaing Division, Myanmar

Maximum Likelihood analysis was conducted using RAxML-VI-HPC v. 8.2.10 (Stamatakis 2014). The most complex model (GTR + Γ) was applied to all partitions, with 1,000 replicate Maximum Likelihood inference runs. We initiated each inference with a random starting tree and assessed nodal support with 1,000 bootstrap pseudoreplicates (Stamatakis et al. 2008). Finally, uncorrected genetic pairwise distances (p-distances) were obtained for the coding region of ND2 (1026 bp, including <31 bp of missing data) using PAUP v. 4.0b10 (Swofford and Sullivan 2003). Nodal support of 70/0.95 or higher for RAxML bootstrap/Bayesian posterior probability, respectively, were considered as strongly supported (Hillis and Bull 1993).

Morphological characters

Morphometric data were taken using a digital caliper to the nearest 0.1 mm, except tail length, which was measured using a thread and a ruler to the nearest 1 mm. Morphometric characters and their measurement methods included the following (abbreviations in parentheses): snout–vent length (**SVL**): measured from tip of snout to anterior edge of cloaca; tail length (**TAL**): measured from the anterior edge of cloaca lip to tip of tail; head length (**HL**): measured from tip of snout to the axis of jaw; head width (**HW**): measured as the linear distance perpendicular to the longitudinal axis of lizard, at the widest point of the head; head depth (**HD**): measured vertically at the jaw; snout–eye length (**SEL**): measured between tip of the snout to the anterior edge of the boney orbit; tympanum diameter (**TD**): measured as the longest diameter of the tympanum, regardless of its direction; eye–tympanum distance (**ETD**): measured between posteroinferior edge of the boney orbit and anterosuperior edge of the tympanum; interorbital distance (**IOD**): measured as the linear distance perpendicular to the longitudinal axis at the widest point between the supraciliary of each side dorsally; orbit diameter (**OD**): measured as the linear distance between the anterior most and the posterior most edge of boney orbit; tallest nuchal crest height (**TNC**): measured from the midpoint of the longitudinal width at the base to the tip of the nuchal crest scale; antebrachium–palm length (**APL**): measured from the elbow to the tip of fourth finger, excluding the claw; brachium length (**BL**): measured from the elbow to the limb insertion point at the axillary; femur length (**FEL**): measured from the knee joint to the limb insertion point at the groin; crust–foot length (**CFL**): measured from the knee joint to the tip of the fourth toe; finger IV length (**F4L**): measured from the base between finger III and IV to the tip of finger IV, excluding the claw; toe IV length (**T4L**): measured from the base between toe III and IV to the tip of toe IV, excluding the claw. Forelimb length (**FLL**) is calculated as the sum of brachium length and antebrachium–palm length, and

hindlimb length (**HLL**) is calculated as the sum of femur length and crust–foot length.

Pholidosis characters and their definitions are the following: supralabial scale count (**SL**): number of elongated labial scales from the rostral to the rictus; infralabial scale count (**IL**): number of elongated labial scales from the mental to the rictus; nasal-supralabial scale row (**NSR**): number of longitudinal scale rows between the nasal and the first supralabial scale; canthus rostralis count (**CR**): number of enlarged, elongated canthus rostralis scales along the canthal ridge from the posterosuperior nasal to and including the last supraciliary; interorbital scale count (**IOS**): number of scales across the transverse straight line between the widest point of the orbit, perpendicular to the longitudinal line; middorsal crest scale count (**MD**): number of crest scales along the longitudinal axis from the head to the point right above cloaca; mid-body scale row around body (**ABR**): number of scale rows around the body at the mid-point between axillary and groin; gular scale count (**GU**): number of enlarged gular scales along the medial longitudinal axis from, and excluding the mental to the neck; ventral scale count (**VN**): number of ventral body scales medial longitudinal axis from and excluding the last gular scale to the last ventral scale anterior to the cloaca; finger IV lamellae scale count (**F4S**): number of subdigital lamellae scales from the base between finger III and IV to the tip of finger IV, excluding the claw; and toe IV lamellae scale count (**T4S**): number of subdigital lamellae scales from the base between toe III and IV to the tip of toe IV, excluding the claw. Additionally, the following morphological characters were examined: gular scale shape (**GulShp**), defined as with elongated tips vs. without tips; neck scale orientation (**NekOrn**), defined as vertically or near vertically (greater than 60° angle) oriented vs. obliquely oriented (less than 60°); axillary scale orientation (**AxlOrn**), size of the mental relative to the first pair of chin shields (**MntChnsld**), dorsolateral color patterns (**DrslClrPat**), and nuchal crest length (**NucL**). Terms for coloration followed Köhler (2012).

Statistical analyses of morphological data

All statistical analyses were conducted using R Core Team (2018). These analyses considered both sexes of four species of the *C. jerdoni* complex (namely *C. jerdoni*, *C. medogensis*, *C. yunnanensis*, and the putative new species). *Calotes maria* were not included in the analyses due to limited sample size. A student t-test revealed sexual dimorphism in most morphometric characters and some meristic characters. As such, males and females were analyzed separately. A Levene's test for the normalized morphometric and meristic characters was conducted to test for equal variances across all groups. Characters with equal variances were analyzed by an analysis of variance (ANOVA) and TukeyHSD post hoc test. Those with unequal variances were subjected to Welch's F-test and Games-Howell post hoc test (Appendix I).

Morphometric characters used in statistical analyses were SVL, TAL, HL, HW, HD, ETD, IOD, SEL, IN, TD, OD, F4L, EN, T4L, FEL, CFL, HLL, BL, APL, FLL, and TRL. In order to most successfully remove the effects of allometry (Chan and Grismer 2022), size was normalized using the following equation: $Xadj = \log(X)-\beta[\log(SVL)-\log(SVLmean)]$, where Xadj = adjusted value; X = measured value; β = unstandardized regression coefficient for each population; and SVLmean = overall average SVL of all populations (Thorpe 1975, 1983; Turan 1999; Lleonart et al. 2000), accessible in the R package GroupStruct (available at https://github.com/chankinonn/GroupStruct). The morphometrics of each species were normalized separately and then concatenated so as not to conflate potential intra- with interspecific variation (Reist 1968; McCoy et al. 2006). All data were scaled to their standard deviation to ensure they were analyzed based on correlation and not covariance.

Meristic characters analyzed were GU, MD, VEN, ABR, F4S, and T4S. Categorical characters for which there was complete coverage for both sexes across all target species were gular scale shape (GulShp), neck scale orientation (NekOrn), axillary scale orientation (AxlOrn), size of mental relative to first pair of chin shields (MntChnsld), dorsolateral color patterns (DrslClrPat), and nuchal crest length (NucL). Sample size for male *C. medogensis* was small (N = 2) so any results from the ANOVA regarding that species should be viewed with caution.

Morpho-spatial clustering and positioning among the species/populations was analyzed using multiple factor analysis (**MFA**) on a concatenated data set comprised of six meristic characters, 20 normalized morphometric characters, and six categorical characters (Appendix II). For this non-parametric multivariate test, it was not necessary to remove the male *C. medogensis* population. The MFA was implemented using the "mfa()" command in the R package FactorMineR (Husson et al. 2017) and visualized using the Factoextra package (Kassambara and Mundt 2017). MFA is a global, unsupervised, multivariate analysis that incorporates qualitative and quantitative data (Pagès 2015) simultaneously, making it possible to analyze different data types in a nearly total evidence environment. In an MFA, each individual is described by a different set of variables (i.e., characters) which are structured into different data groups in a global data frame—in this case, quantitative data (i.e., meristics and normalized morphometrics) and categorical data (i.e., scale, tubercle, and caudal morphology). In the first phase of the analysis, separate multivariate analyses are carried out for each set of variables—principal component analyses (**PCA**) for each quantitative data set and a multiple correspondence analysis (**MCA**) for the categorical data. The data sets are then normalized separately by dividing all their elements by the square root of their first eigenvalue. For the second phase of the analysis, these normalized data sets are concatenated into a single matrix for a final global PCA of the normalized data. Standardizing the data in this manner prevents one data type from overleveraging another. In other words, the normalization of the data in the first phase prevents data types with the most number

of characters or the greatest amount of variation from outweighing other data types in the second phase. This way, the contributions of each data type to the overall variation in the data set are scaled to define the morphospatial distance between individuals as well as calculating each data type's contribution to the overall variation in the analysis (Pagès 2015; Kassambara and Mundt 2017).

A non-parametric permutation multivariate analysis of variance (PERMANOVA) from the vegan package 2.5-3 in R (Oksanen et al. 2020) was used to determine if the centroid locations and group clustering of each species/population in the MFA were statistically different from one another (Skalski et al. 2018). The analysis was based on the calculation of a Gower (dis)similarity matrix using 50,000 permutations based on the loadings of the first four dimensions of the MFA. A pairwise post hoc test calculates the differences between all combinations of population pairs, generating a p-value, a Bonferroni-adjusted p-value, and a pseudo-F ratio (F statistic). A value of $p < 0.05$ is considered significant and larger F statistics indicate more pronounced group separation. A rejection of the null hypothesis (i.e., centroid positions and/or the spread of the data points, i.e., clusters, are not different from random) signifies a statistically significant difference between species/populations.

Results

Molecular results

The *C. jerdoni* complex was recovered as a monophyletic group within the genus *Calotes* (bootstrap support 100/Bayesian posterior probability 1.00, herein abbreviated in this order; Fig. 2). The topotype of *C. jerdoni* and the individual from Nagaland were recovered as monophyletic with strong support (100/1.00), and sister to the individual from western Myanmar with low support (62/0.62). Individuals from southwestern Yunnan and *C. medogensis* formed sister clades (100/1.00), with strong support (89/1.00) (Fig. 2).

The topotypic *C. jerdoni* showed considerable genetic divergence from the western Myanmar individual based on 1026 bp of ND2 coding region (11.6%). Moreover, the Yunnan individuals also showed considerable genetic divergence from topotypic *C. medogensis* (14.0–14.2%) but minimal divergence among themselves (0.1–1.4% among Yunnan individuals; 0.1% among topotypic *C. medogensis*; Table 2).

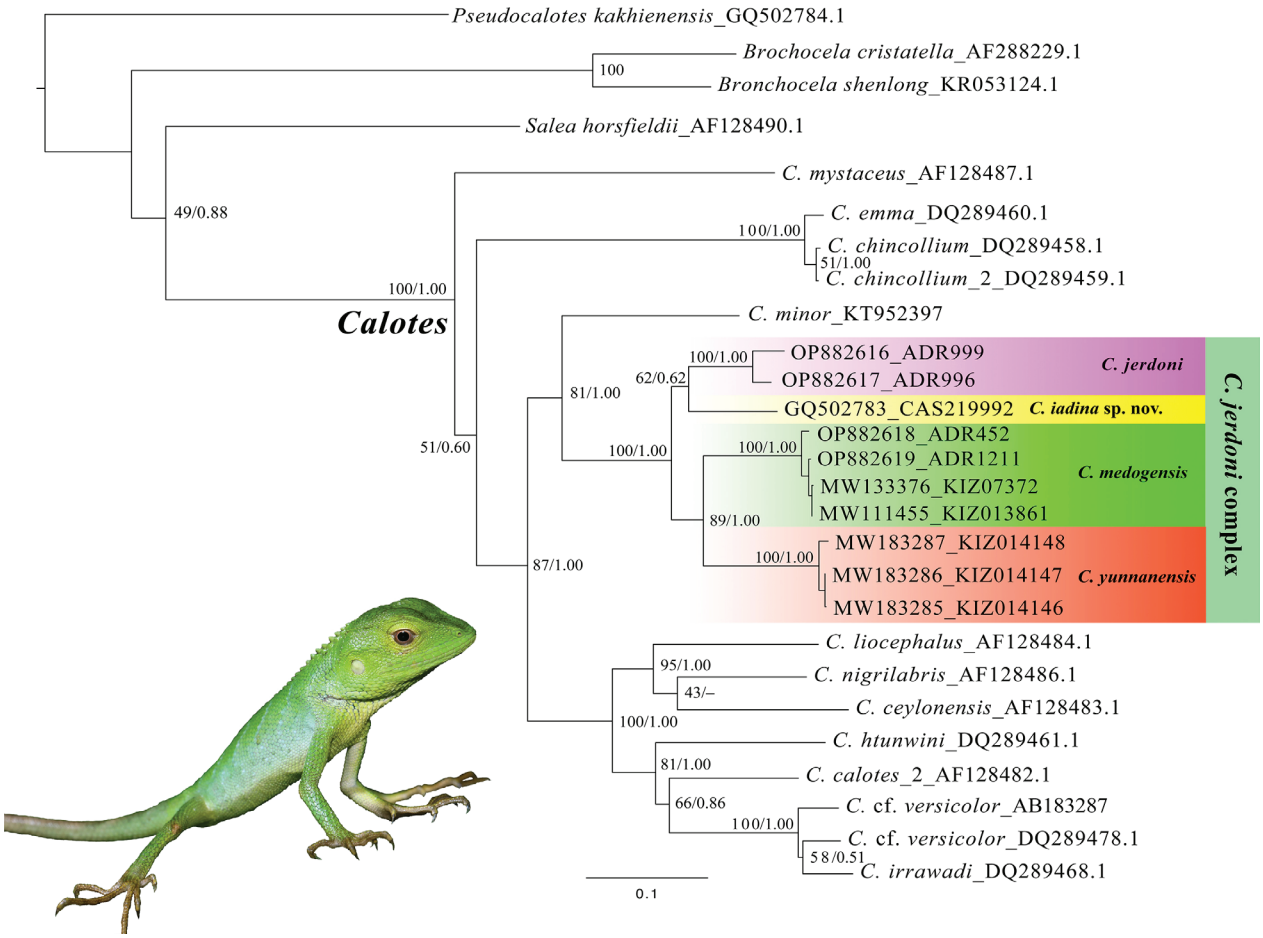

Figure 2. Mitochondrial genealogy of *Calotes jerdoni* complex derived from ND2 dataset using Bayesian and Maximum Likelihood methods. Bayesian posterior probabilities were mapped on the Maximum Likelihood topology, where the unresolved polytomy were noted as "–". Each sequence name is formatted as GenBank succession number followed by its associated voucher number. The color of major clades of *C. jerdoni* correspond to those used in Figure 1. The inserted image of *C. medogensis* was taken by Jian Wang.

Table 2. Uncorrected genetic distances (in unit of %) of members of the *Calotes jerdoni* complex and selected congeners based on 1023 bp of ND2 coding region.

	Species	1	2	3	4	5	6	7	8	9	10	11
1	*C. mystaceus* AF128487	—										
2	*C. jerdoni* topotype OP882616	25.6	—									
3	*Calotes iadina* **sp. nov.** GQ502783	25.9	11.6	—								
4	*C. medogensis* topotype MW133376	24.6	14.7	14.3	—							
5	*C. medogensis* topotype MW111455	24.6	14.6	14.2	0.1	—						
6	*C. yunnanensis* topotype MW183287	24.3	15.1	14.5	14.1	14.0	—					
7	*C. yunnanensis* topotype MW183285	24.5	14.7	14.2	14.2	14.1	1.4	—				
8	*C. yunnanensis* topotype MW183286	24.5	14.8	14.1	14.1	14.0	1.3	0.1	—			
9	*C. liocephalus* AF128484	23.7	21.7	21.0	22.1	22.2	22.8	22.6	22.5	—		
10	*C. ceylonensis* AF128483	23.4	21.7	22.3	23.5	23.4	23.8	23.7	23.6	18.3	—	
11	*C. nigrilabris* AF128486	23.0	22.9	23.9	23.5	23.4	22.8	23.0	23.0	17.2	16.5	—

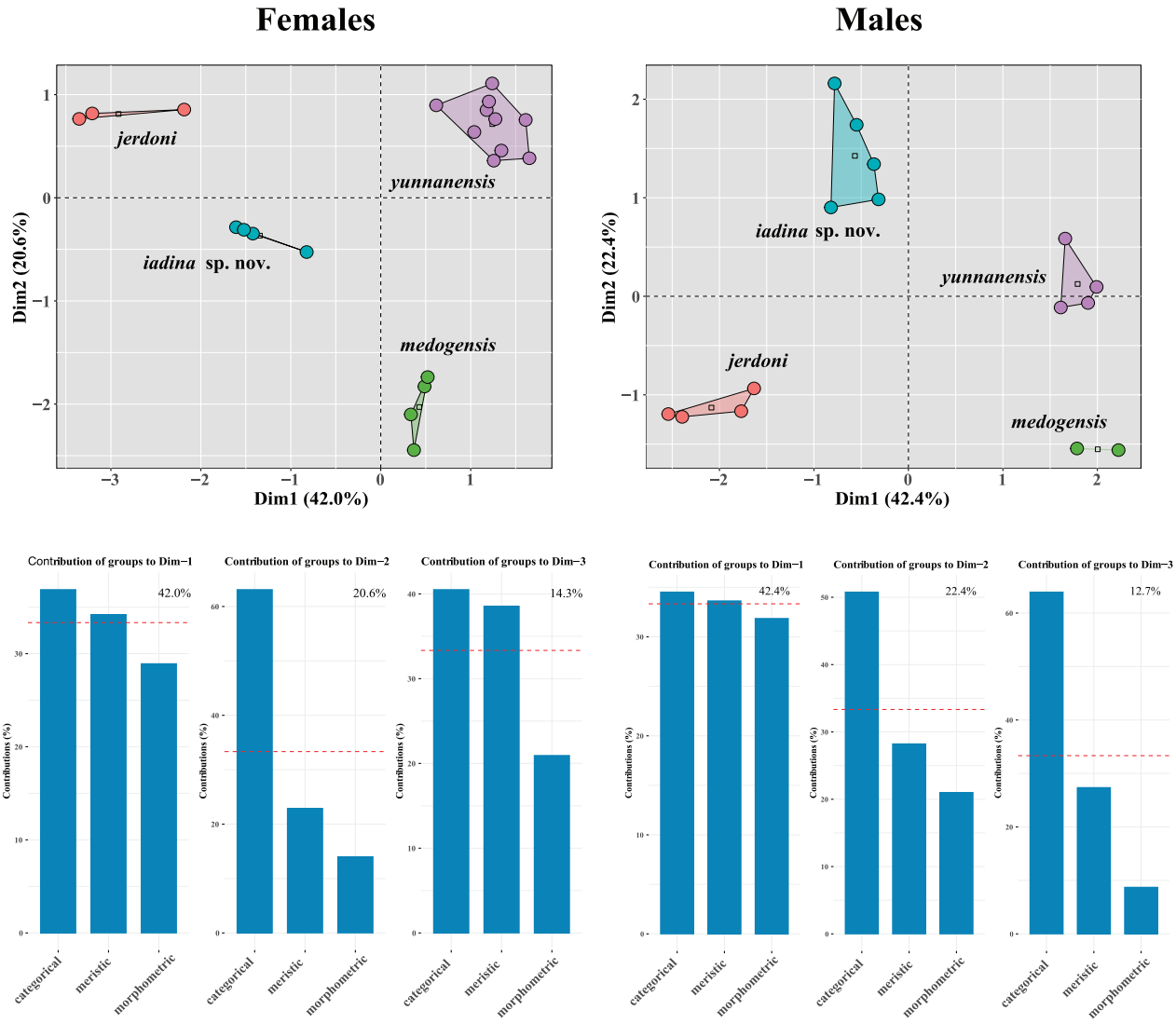

Figure 3. Female and male MFA plots of the four target species and bar plots of the percent contribution of each data type to Dim 1–3 of the MFA. The percentage score at the top of each bar plot is the percent contribution of that dimension to the overall variation in the data set. The red dotted lines in the bar plots represent the mean percentage values.

Morphological results

The females from the Nat Ma Taung National Park in Myanmar plotted separately in the MFA with the categorical and morphometric data contributing most to the total inertia (42.0%) of dimension 1, categorical data contributing most to the total inertia (20.6%) of dimension 2, and meristic and categorical data contributing most to

Table 3. Morphological comparisons among members of the *Calotes jerdoni* complex. Abbreviations, see "Materials and methods" section. "–" indicates missing data, and "*" indicates different sample size due to damaged specimen or missing data. Values of main diagnostic characters are in bold.

Species	***Calotes jerdoni***		***C. iadina* sp. nov.**		***C. yunnanensis***		***C. medogensis***		***C. maria***	
Sex	**M**	**F**	**M**	**F**	**M**	F	M	F	M	F
Sample Size	3*	3	5	4	3	11*	2	4	2	2
SVL	65.8–76.6 (72.6)	74.04–102.2 (88.3)	63.2–102.5 (78.7)	71.1–97.0 (82.4)	67.8–80.6 (74.7)	73.8–102.8 (90.7)	75.7–76.4 (76.1)	86.2–95.8 (84.7)	101.0–117.5 (109.3)	102.0–109.6 (105.8)
TAL/SVL (%)	**276.6–318.6 (290.3)**	**271.0–324.4 (290.3)**	302.3–368.0 (346.7)	293.9–325.6 (313.6)	319.7–341.4 (328.8)	292.0–346.6 (328.5)*	286.7 (–)*	297.8–326.1 (314.5)	318.3–318.8 (318.6)	318.6–323.9 (321.3)
TRL/SVL (%)	46.6–55.3 (51.5)	49.9–54.3 (51.7)	47.4–50.6 (49.1)	50.5–52.3 (51.2)	46.1–46.7 (46.4)	45.5–55.5 (50.2)	45.6–48.7 (47.2)	41.4–50.8 (47.2)	45.3–46.1 (45.7)	50.2–50.3 (50.2)
HW/HL (%)	61.6–66.7 (64.3)	61.0–68.6 (65.7)	56.6–62.7 (59.7)	59.9–61.4 (60.6)	60.1–63.6 (61.4)	59.9–66.5 (62.0)	58.7–59.0 (58.9)	58.4–61.6 (60.1)	18.3–18.9 (18.6)	19.8–20.2 (20.0)
HD/HL (%)	55.4–59.7 (56.9)	52.3–55.9 (55.2)	51.9–56.4 (53.4)	53.7–54.9 (54.2)	52.0–53.5 (52.7)	46.6–58.1 (52.6)	50.9–51.6 (51.2)	49.0–52.1 (50.7)	48.8–54.9 (51.8)	53.4–55.1 (54.2)
TD/ED (%)	30.7–50.2 (39.4)	32.7–46.0 (40.8)	37.2–49.7 (43.1)	41.3–46.3 (44.6)	37.2–58.5 (48.7)	37.3–66.0 (51.2)	44.0–52.6 (48.3)	47.4–55.0 (51.7)	39.2–40.0 (39.6)	40.3–52.7 (46.5)
FLL/SVL (%)	58.1–59.1 (58.6) *	47.8–57.8 (53.7)	51.6–60.4 (57.6)	52.9–59.3 (56.0)	53.1–61.2 (58.1)	50.9–58.8 (56.1)*	55.4–57.7 (56.6)	53.2–62.4 (58.6)	52.2–56.0 (54.1)	58.4–59.3 (58.9)
HLL/SVL (%)	82.9–85.3 (84.1)*	71.6–83.4 (78.5)	76.2–88.4 (84.3)	77.3–87.0 (82.5)	80.0–86.0 (83.7)	73.4–88.6 (83.2)*	78.2–80.3 (79.2)	79.5–89.0 (84.7)	78.8–79.1 (79.0)	84.9–90.7 (87.8)
TNC/HL (%)	8.1–10.5 (9.3)*	10.1–13.2 (11.3)	8.3–13.3 (11.4)	10.4–11.3 (10.8)	14.1–16.9 (15.4)	14.8–21.2 (17.5)*	**5.2–7.3 (6.3)**	10.3–15.7 (12.6)	**19.1–19.5 (19.3)**	**17.6–24.0 (20.8)**
MD	34–40 (37)		38–43 (42)		38–42 (41)		39–42 (40)		**47–52 (49)**	
GU	16–19 (18)		16–19 (18)		21–25 (24)		20–25 (23)		27–31 (30)	
VN	62–75 (72)*		**48–54 (51)**		54–68 (61)		57–61 (59)*		63–76 (72)	
ABR	46–53 (49)*		45–53 (50)		50–58 (54)		**54–60 (57)***		**58–67 (62)**	

the total inertia (14.3%) of dimension 3 (Fig. 3). The PERMANOVA analysis recovered the morphospatial position of the Nat Ma Taung National Park females being statistically different from the positions of the females of *C. jerdoni*, *C. medogensis*, and *C. yunnanensis* (Appendix I). The ANOVA analyses recovered the female population from Nat Ma Taung National Park as having significantly different mean values for several characters from all other species (Appendix II).

The males from the Nat Ma Taung National Park in Myanmar plotted separately in the MFA with all the data types contributing nearly equally to the total inertia (42.4%) of dimension 1, morphometric data contributing most to the total inertia (22.4%) of dimension 2, and categorical data contributing most to the total inertia (12.7%) of dimension 3 (Fig. 3). The PERMANOVA analysis recovered the morphospatial position of the Nat Ma Taung National Park males being statistically different from the positions of the males of *C. jerdoni*, *C. medogensis*, and *C. yunnanensis* (Appendix III). The ANOVA analyses recovered the male population from Nat Ma Taung National Park in Myanmar as having significantly different mean values for several characters from all the other species (Appendices IV, V).

Morphological comparisons

The western Yunnan population of *C.* cf. *jerdoni* is morphologically identical to the northern and eastern Myanmar population (Table 3). For the remaining populations, while overall similar, different clades of *C. jerdoni* complex show statistically significantly distinct morphological characters that can be readily differentiated (Appendix V). Specifically, the original syntype series and topotypes of *C. jerdoni* can be differentiated from the remaining members of the complex by having axillary scales oriented straight posteriorly or posterosuperiorly at an angle less than 60° (vs. axillary scales oriented vertically or near vertically); and from the Yunnan /the northern and eastern Myanmar populations and *C. medogensis* by having larger and fewer gular scales along central midline (GU larger, 16–19 vs. smaller, > 20) and by having a distinctively elongated tip of each gular scale (vs. short or no elongated tip; Fig. 4).

The western Yunnan/northern and eastern Myanmar populations are morphologically most similar to *C. medogensis*, but they can still be differentiated by having longitudinally oriented keels on the head scales posterolateral to parietal scale (vs. transversely oriented), longer nuchal crests (TNC 14.8–21.2% vs. 5.2–15.7%), larger mental scale relative to the chin shields (vs. smaller or barely equal sized), and more distinctively keeled gular scales, particularly on posterolateral region (keel extending across the entirety individual scale vs. only extending across posterior half or less; Fig. 4).

Calotes medogensis can be readily diagnosed from *C. maria* by a combination of morphological characters, including the presence of a shoulder fold (vs. absence), larger and fewer gular scales (GU 20–25 vs. 31), crest scales (MD 39–42 vs. 52), and dorsal and ventral body scales (ABR 54–60 vs. 67; VEN 57–61 vs. 75). Furthermore, *C. medogensis* differs from *C. maria* by having a tympanum that is farther away from the parallel ridges of the head (1 or 2 scales away vs. 3 or 4 scales), transversely oriented keels on the head scales posterolateral to parietal scale (vs. longitudinally oriented) and by having a different shape and size of the scales on the parallel ridges (posteriormost few scales slightly enlarged and in conical shape vs. distinctively elongate into spine shape) (Fig. 4).

Given the considerable genetic divergences, monophyletic nature, and conservative morphological diagnoses, we consider the Yunnan/northern and eastern Myanmar population and the western Myanmar populations of *C.* cf. *jerdoni* as two distinct species. As the Yunnan/northern and eastern Myanmar population has an available junior synonym, *C. yunnanensis*, we resurrect this synonym as a valid nomen for this species. For the western Myanmar population, we describe it as a new species. Additionally, with the clear morphological differentiation, our data support *C. medogensis* as a valid species with respect to *C. maria*, and we redescribe both species based on type material.

Taxonomic accounts

The following four species are diagnosed as members of the *C. jerdoni* complex by having (1) two parallel rows of conical/spinous scales from the posterior of the eye to the temporal region of the head, with a superior row continuing from the supraciliaries and an inferior row from the posteroinferior margin of the eye, with both terminating in the squamosal region of head; and (2) a green dorsal background coloration.

Calotes jerdoni Günther, 1870

Appendix VI

Lectotype. NHMUK 1946.8.11.54, adult male from Khasi Hill, India.

Paralectotypes examined. NHMUK 1946.8.50., adult male; NHMUK 1946.8.11.49, NHMUK 1946.8.11.51, NHMUK 1946.8.11.53, NHMUK 1946.8.11.56, adult females. Same collection information as the lectotype.

Expanded Diagnosis. *Calotes jerdoni* can be diagnosed from members of the species complex by a combination of following morphological characters: (1) body size large, SVL 65.7–102.2 mm; (2) tail slender, long, TAL 271.0–324.3% SVL; (3) posterior-most conical scales of parallel ridges of head not elongated into spine shape, relatively low; (4) inferior row of conical scales 1 or 2 scales away from superior tympanum, TRD 38.4–52.5% TD; (5) scales posterolateral of parietal bearing longitudinal keels; (6) gular scales large, 16–19 along central midline, homogeneous in posteromedial region, much larger than ventrals; (7) gular scales strongly keeled, mucronate with distinct, elongated tips; (8) distinct gular pouch absent, transverse gular fold absent; (9) body scales large, ABR 46–53; (10) shoulder fold present, short, covered with granular scales underneath; (11) neck scales oriented straight posteriorly; (12) axillary scales oriented posteriorly or posterosuperiorly at an angle less than 60°; (13) nuchal crests relatively short, triangular shaped, differentiated from dorsal crest, TNC 8.1–13.2% HL; (14) middorsal crest scale count 34–40; (15) scale rows around midbody 46–53; (16) ventral scale count 62–75, (17) F4S 19–26, T4S 25–31; (18) dorsal and ventral background coloration Yellow Green (Color 103) to Grass Green (Color 110) in normal condition, can change drastically to dark brown to blackish red under stress; (19) Medium Chrome Orange (Color 75) patches present on elbows, knees, and ankles; and (20) Pale Pinkish Buff (Color 3) to Medium Chrome Orange (Color 75) dorsolateral stripes from neck to basal tail present in some individuals.

Calotes maria Gray, 1845

Figures 4–6; Appendix VI

Synonymy.
Calotes platyceps Blyth, 1852: 354

Lectotype. NHMUK 1946.8.11.24, adult male from "Afghanistan" (see remarks on its type locality below); designated by Boulenger (1885).

Additional examined specimens. NHMUK 1870.11.29.30a, adult male; 1870.11.29.30b, adult female; both from Khasia (Khasi Hill), India; NHMUK 1860.3.19.1020, adult female from "Afghanistan".

Remarks on its type locality and type specimens. On its original description, Gray (1845) described the species based on four specimens: three individuals (a juvenile, a subadult, and an adult) from "Affghanistan and a single half-grown individual from Khassia Hill". Later Boulenger (1885) designated a male from Affghanistan as the "type" (= lectotype) of *C. maria* (NHMUK 1946.8.11.24), and he identified two of the young male syntypes of *C. maria* as *C. jerdoni*.

Based on Blyth (1853), the initial syntypes of *C. maria*, along with other species of the genus *Calotes*, were collected by Dr. Griffith and later handled by the East India Company before donating them to the Natural History Museum. Blyth (1853) suspected that those specimens from "Affghanistan" (= Afghanistan) and "Khassia Hills" (= Khasi Hill) were mixed during the handling by the East India Company. As the tropical species *C. ma-*

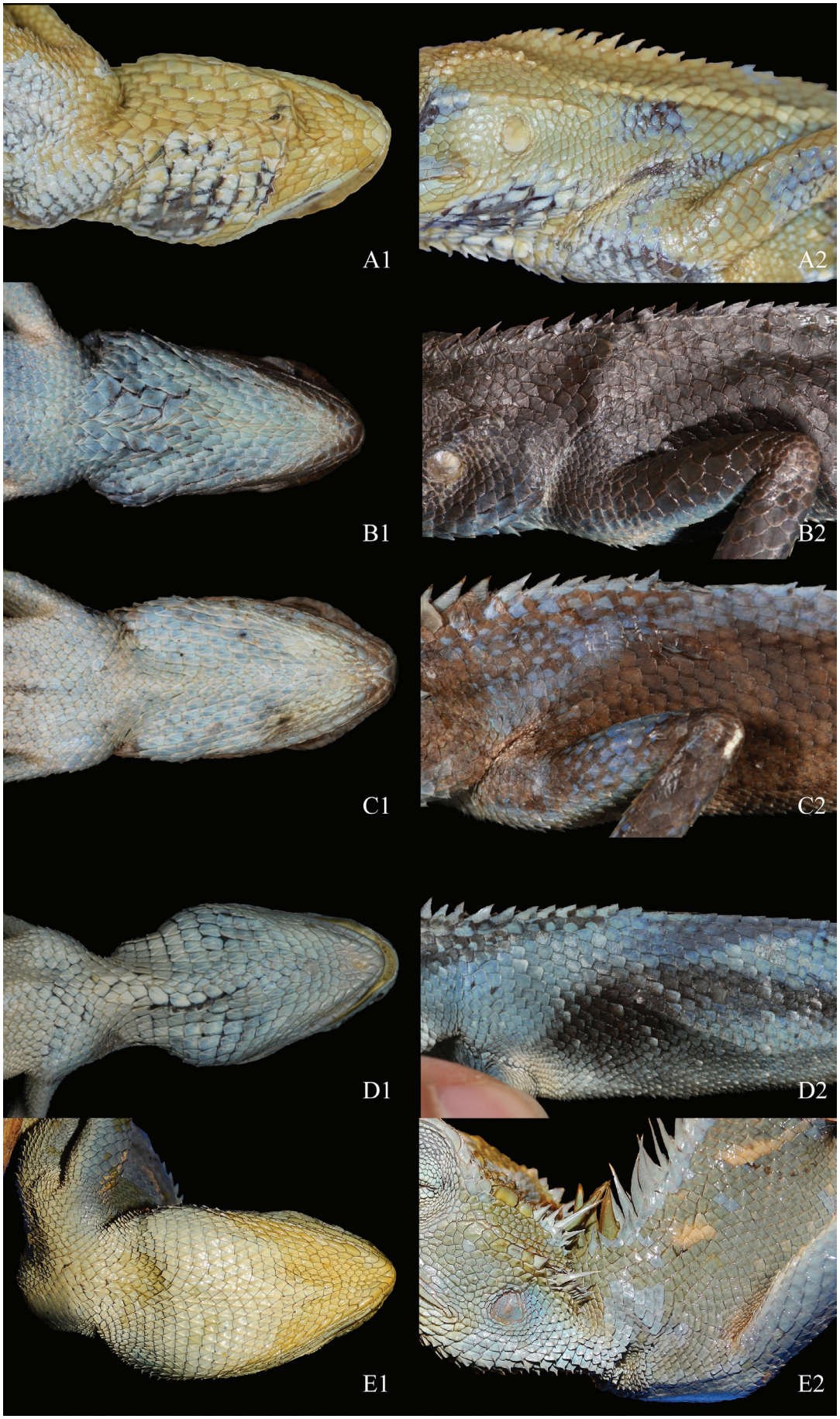

Figure 4. Morphological comparison among *C. jerdoni* (**A**) (NHMUK 1946.8.11.54), *C. iadina* **sp. nov.** (**B**) (CAS 219992), *C. yunnanensis* (**C**) (KIZ 014148), and *C. medogensis* (**D**) (KIZ 019546), and *C. maria* (NHMUK 1946.8.11.24), showing characteristics of the gular scales (1) and axillary scales (2). Photos by V. Deepak and Kai Wang.

ria certainly cannot survive in desert or cold highlands of Afghanistan, and given Afghanistan is zoogeographically distinct from northeast India, the type locality of *C. maria* was certainly mistaken as Afghanistan and should be replaced by "Khassia Hills", which refers to the Khasi Hill in Meghalaya State, Northeast India.

Remarks on the "synonym" *C. platyceps*. First described in 1852, *C. platyceps* was described in a short, rather simple description without a clear statement regarding its type specimen. Later, based on specimens collected from Khasi hills, Jerdon (1870) identified his specimens as *C. platyceps* and added a diagnosis of *C. platyceps* against *C. maria*, including a smaller body size, larger and fewer gular and body scales, and a narrower distance between supratympanic crest and the upper edge of tympanum. While the diagnosis of "*C. platyceps*" described by Jerdon (1870) matches the diagnosis of *C. jerdoni*, they were not based on the type specimen of *C. platyceps*. Subsequently, Boulenger (1885) without explanation, considered *C. platyceps* a junior synonym of both *C. maria* and *C. jerdoni*—a taxonomic treatment followed by subsequent authors (Boulenger 1890; Smith 1935; Che et al. 2020; Uetz et al. 2023).

Although the presence of a supratympanic crest on each side of the head aligns *C. platyceps* with the *C. jerdoni* complex, based on the limited information in the original morphological description, it is impossible to confirm whether *C. platyceps* represents a junior synonym of *C. maria* or *C. jerdoni*. As the type specimen of *C. platyceps* cannot be located, and since the original description of the species provides little useful information on its taxonomic identity, we treat the name *C. platyceps* as a nomen dubium. As such, the name is nomenclaturally still available, but it has no bearing on the taxonomic and nomenclatural decisions made here.

Diagnosis. *Calotes maria* can be diagnosed from its congeners by a combination of following morphological characters: (1) body size large, SVL 101–117.5 mm; (2)

Figure 5. Lectotype of *Calotes maria* (NHMUK 1946.8.11.24), showing dorsal (**A**), ventral (**B**), lateral head (**C**), ventral head (**D**), dorsal head (**E**), and axillary region (**F**). Photos by V. Deepak.

Figure 6. Non-vouchered individuals of *Calotes maria* in life, showing an adult (**A**) from Royal Manas National Park and a juvenile (**B**) from Garo Hill, Meghalaya. Photos by Abhijit Das.

tail slender, long, TAL 318.3–323.9% SVL; (3) posterior-most conical scales of parallel ridges of head distinctively elongated into spine shape, about same length as longest nuchal crest; (4) inferior row of conical/spinous scales 4 scales away from superior tympanum; (5) dorsal head scales posterolateral of parietal bearing longitudinal keels; (6) mental smaller than first pair of chin shields; (7) gular scales count 27–31, homogeneous in posteromedial region, much larger than ventrals, mucronate with distinct, moderate-lengthed tips; (8) body scales small, ABR 58–67; (9) distinct gular pouch absent, transverse gular fold absent; (10) shoulder fold absent; (11) neck scales oriented posterosuperiorly; (12) axillary scales oriented posterosuperiorly at an angle less than 60°; (13) nuchal crests long, elongated, lanceolate-shaped, differentiated from dorsal crest, TNC 17.6–24.0% HL; (14) middorsal crest scale count 47–52; (15) ventral scale count 63–76, (17) F4S 23–28, T4S 28–32; (18) dorsal background coloration Pratt's Payne's Gray (Color 293) to Sky Blue (Color 192) under long-term preservation, ventral Paris White (Color 139); and (19) short, Pale Pinkish Buff (Color 3) to Yellow Ocher (Color 14), oblique stripes present on dorsum, similar colored patches present on tail base.

Redescription of the lectotype. Large sized *Calotes*, SVL 101.0 mm; body not compressed dorsally, lachrymiform in cross-section; tail swollen at base, long, TAL 322 mm, 318.8% SVL. Limbs slender, forelimb 52.7 mm, 52.2% SVL; hindlimb 69.8 mm, 69.1% SVL. Rostral rectangular, bordering four small scales excluding supralabials; supralabials 10/11, feebly keeled posteriorly; nasal elongated oval, bordering second supralabial, 6/7 scales away from orbit circle; loreals distinctively keeled, each bearing single keel; canthal ridge distinct, canthus rostralis scales 10/10, elongated except anterior most two, supraciliaries only slightly overlapping, overlapping length less than half of scale length; suborbital scale rows 3/3, about equal size, each scale bearing single, distinct, inferior-located lateral keel. Distinctively protruding, enlarged keeled scales each bearing multiple keels aligned in two parallel lateral ridges: superior row continuing from posterior most supraciliary to superior squamosal head, consisting 8 raised scales, anterior-most 2 and 4 scales conical on left and right, respectively, remaining 6 and 4 much more elongated into spikes; inferior row two small scales away from posterior mid orbit to inferior squamosal head, consisting 12/10 scales, anterior-most 5 sub-pyramidal or conical, remaining posterior scales elongated into spikes. Inferior one of parallel ridges four small scale rows away from anterior tympanum. Tympanum exposed, round, TD 10.5% HL; no post orbital spikes, posterosuperior tympanic and temporal spikes present, which are located on parallel ridges. Dorsal head scales heterogeneous in size and shape, slightly larger above eyes, distinctively smaller on temporal, moderately keeled, each bearing single keel; enlarged scales arranged in Y-shape three scales posterior to rostral along longitudinal midline, with posterior most scale on stem of "Y" figure largest; 17 scales transversely across dorsal head between and excluding supraciliary at widest point; parietal scale elongated, narrow, parietal eye present; scales posterolateral of parietal bearing longitudinal keels.

Except scales anterior to shoulder, all dorsal body scales broad triangular shaped, regularly arranged, imbricate, mostly homogeneous, weakly keeled; neck scales oriented posterosuperiorly; axillary scales oriented posterosuperiorly; remaining lateral and superior body scales oriented posterosuperiorly, inferolateral body scales more distinctively keeled, oriented straight posteriorly or inferoposteriorly; midbody scale row around body 67. Nuchal crest 13, distinctively elongated into spikes, much taller than remaining dorsal crests, tallest one 5.6 mm in height, 19.5% HL; dorsal crests much lower, curving posteriorly; mid-dorsal crest scale count 52 anterior to cloaca; shoulder fold absent. Scales of dorsal limbs more or less homogeneous, keeled. Dorsal tail scales homogeneous, feebly keeled or smooth anteriorly, more distinctively keeled posteriorly.

Mental spear-shaped, enclosed by and smaller than first pair of chin shields; chin shields feebly keeled, larger than nearby gulars, 5/6, anterior most 3/2 in contact with infralabials on each side, remaining ones separated by one or two rows of small scales; infralabials 10/10, more distinctively keeled than supralabials; gular scales all distinctively keeled; anterior gulars smaller, juxtaposed, various in shape and size; remaining posterior gular scales larger, similar size to dorsals, rhomboid shaped, imbricated, mucronate with moderate-length tip on posterior end of each gular; post mental gular scales 30 along medial line. Ventral body cut open from chest to pelvis, ventral scales imbricated, slightly smaller than larger gulars, distinctively keeled, carinated, ventral scale count 76 along medial axis from neck to cloaca. Ventral limb scales homogeneous in size, more distinctively keeled than dorsal limb scales; subdigital lamellae 27/28 under finger IV, 32/32 under toe IV. Tail scales distinctively keeled, carinated (ventral tail cut open at base).

Calotes medogensis Zhao & Li, 1984

Figures 4, 7, 8, Table 3; Appendix VI

Holotype. CIB 1477/8380177, adult male from Yarang, Medog County, Nyingchi Prefecture, Xizang Autonomous Region, China.

Additional examined specimens. KIZ 014003, 019546, adult females; KIZ 013861, subadult female; all from Beibeng, Medog County, Nyingchi Prefecture, Xizang Autonomous Region, China.

Referred specimens. WII-ADR 1211, WII-ADR 452, both adult females from the East Himalaya (Boruah et al. 2022).

Diagnosis. *Calotes medogensis* is diagnosed from congeners by a combination of the following characters: (1) body size large SVL 75.7–95.9 mm; (2) tail slender, long,

TAL 286.7–326.1% SVL; (3) conical scales forming two parallel ridges from posterior eye to temporal head, posterior most 3–5 scales of superior ridge distinctively raised and conical, but not elongated into spikes; (4) inferior ridge of conical scales 2–3 scale-rows away from superior tympanum, TRD 36.9–63.2% TD; (5) dorsal head scales posterolateral of parietal bearing transverse keels; (6) mental smaller than first pair of chin shields; (7) gular scale count 20–25 along central medial line, larger than ventrals, mucronate with feeble tips; (8) gular scales keeled, but keel often extending less than ½ of scale length on posterolateral region; (9) gular pouch present in life, weakly developed, but absent after preservation; (10) transverse gular fold absent; (12) shoulder fold present, short, covered with granular scales underneath; (13) nuchal crests relatively short, lanceolate shape, dorsal crests moderately developed, TNC 5.2–7.3% HL in males, 10.3–15.7% in females; (14) neck scales oriented posterosuperiorly, larger than ventrals; (15) axillary scales oriented near vertically; (16) middorsal crest scale count 37–42, (17) scale rows around midbody 53–60; (18) ventral scale count 57–65; (19) F4S 25–29, T4S 30–34; (20) dorsal and ventral background coloration Yellow Green (Color 103) to Grass Green (Color 110) in normal condition, can change drastically to dark brown to blackish under stress; (21) region underneath shoulder fold Dark Carmine (Color 61) to Poppy Red (Color 63); (22) white to Medium Paris White (Color 140), narrow, oblique streaks present on lateral dorsum, running anterosuperiorly to posteroinferiorly, each streak formed by a single row of scale.

Redescription of holotype. Medium sized *Calotes*, SVL 75.7 mm, body not compressed dorsally, lachrymiform in cross-section; tail complete, swollen at base, long, TAL 217 mm, 286.7% SVL. Limbs slender, forelimb 42.0 mm, 55.4% SVL; hindlimb 59.2 mm, 78.2% SVL. Rostral rectangular, bordering six small scales excluding supralabials; supralabials 11/11, feebly keeled posteriorly; nasal elongated oval, bordering second supralabial, six scales away from orbit circle; loreals distinctively keeled, each bearing single longitudinal keel; canthal ridge distinct, canthus rostralis scales 10/11, elongated except posterior most two, supraciliaries only slightly overlapping, overlapping length one third of scale length; suborbital scale rows 4/4, scales about equal size, each bearing single distinct lateral keel. Distinctively protruding, enlarged keeled scales each bearing single lateral keel aligned laterally in two parallel ridges: superior row continuing from posterior most supraciliary to superior squamosal head, consisting of 9/10 conical scales; inferior row from posterior mid orbit to inferior squamosal head, consisting of 10/10 scales, anterior five sub-pyramidal, posterior most four conical. Inferior ridge two small scale rows away from anterior tympanum. Tympanum exposed, round; no post orbital, posterosuperior tympanic, or temporal spikes. Dorsal head scales heterogeneous in size and shape, distinctively keeled, each bearing single longitudinal keel except ones on temporal, which bearing single transverse keel; enlarged scales arranged in Y-shape four scales posterior to rostral along longitudinal midline, with posterior most scale on each opening branch of "Y" figure largest; 17 scales transversely across dorsal head between supraciliary at widest point; parietal scale enlarged, spear-shaped pointing posteriorly, parietal eye distinct; scales posterolateral of parietal bearing transverse keels.

Except scales beneath shoulder fold, all dorsal body scales broad, triangularly shaped, regularly arranged, imbricate, homogeneous, weakly keeled; neck scales oriented posterosuperiorly; axillary scales oriented vertically upward; remaining lateral and superior body scales oriented posterosuperiorly, inferolateral body scales more distinctively keeled, oriented straight posteriorly; midbody scale row around body 46. Nuchal crest low trian-

Figure 7. Holotype of *Calotes medogensis* (CIB 1477/8380177), showing dorsal (**A**), ventral (**B**), lateral head (**C**), ventral head (**D**), dorsal head (**E**), and axillary region (**F**). Photos by Kai Wang.

gular shaped, slightly damaged, ninth nuchal crest tallest, 1.2 mm in height, 1.0 mm in longitudinal width at base; nuchal crest gradually transitioned to lower, serrated dorsal crest posteriorly; mid-dorsal crest scale count 40 anterior to cloaca; distinct shoulder fold present, short, with fine granular scales underneath. Dorsal scales of dorsal limbs homogeneous, slightly larger on distal appendages, keeled. Tail scales homogeneous, feebly keeled, or smooth anteriorly, more distinctively keeled posteriorly.

Mental pentagonal, not enclosed by and smaller than first pair of chin shields; chin shields smooth anteriorly, feebly keeled posteriorly, slightly enlarged than nearby gulars, 6/6, anterior most 2 in contact with infralabials on each side, remaining ones separated by one or two rows of small scales; infralabials 11/12, feebly keeled; gular scales all distinctively keeled; anterior gulars small, juxtaposed, various in shape and size; remaining posterior gular scales larger, similar size to dorsals, rhomboid shaped, more homogeneous, imbricated, keel of individual scale only extending less than half of scale length; posterior gular scales slightly mucronate with feeble tips; post mental gular scales 23 along medial line. Ventral body scales imbricated, smaller than gulars and dorsals, distinctively keeled, carinated, ventral scale count 58 along medial axis from neck to cloaca. Ventral limb scales homogeneous in size, more distinctively keeled than dorsal limb scales; subdigital lamellae 29/27 under finger IV, 34/31 under toe IV. Ventral tail scales distinctively keeled, carinated.

Description of coloration in life. The lateral sides of head are uniformly Yellow Green (Color 103). The dorsal surface of the head is darker than lateral sides, which are Light Grass Green (Color 103). Lateral sides of the head gradually transition to Pistachio (Color 102) or Light Grass Green (Color 103) posteriorly to the dorsal and lateral dorsum, and further inferiorly to Pale Cyan (Color 156) on ventrolateral dorsum. The region underneath the shoulder fold is Dark Carmine (Color 61) to Poppy Red (Color 63). Most individuals have white to Medium Paris White (Color 140) oblique streaks that run anterosuperiorly to posteroinferiorly, and each streak is formed by a single row of scale. The ventral surfaces of the head and body are uniform Yellow Green (Color 103). Some individuals have a small patch on the knee and ankle, respectively, which is Orange-Rufous (Color 56) in color.

Natural history and conservation. *Calotes medogensis* is arboreal, inhabiting tropical forests at mid to low elevations, and individuals were observed sleeping on twigs

Figure 8. Topotypic individuals of *Calotes medogensis* in life. KIZ 07372 (**A**), KIZ 014003 (**B**), unvouchered individuals (**C–G**). Photos by Kai Wang and Jian Wang.

and vines less than 2 m above the ground at night. *Calotes medogensis* is an insectivore, feeding on various beetles and other insects. Currently, the species is known from Medog County, Xizang Autonomous Region, China and the adjacent region in northeastern India (Boruah et al. 2022). In Medog, *C. medogensis* is sympatric with other agamids such as *C. paulus*, *Japalura andersoniana*, and *Mictopholis austeniana*. Possible predation may come from lizard-feeding snakes such as *Lycodon* cf. *fasciatus*, *Oligodon* spp., and *Ptyas nigromarginata* (Che et al. 2020). One of the voucher females (KIZ 014003) is gravid with 11 eggs. With no pressing threats and protection coverage by nature reserves in both China and India, we propose to list the species as Least Concern (LC) for China's Red List Assessment and IUCN Assessment.

Calotes iadina Wang, Deepak & Grismer sp. nov.

https://zoobank.org/5BFD358A-B843-413A-B4AB-931536B89F97

Figures 4, 9, 10, Table 3, Appendix VII

Chresonymy.
Calotes jerdoni – Zug et al. (2006: 60)

Holotype. CAS 219992, adult male from Baw Khue Plantation, Nat Ma Taung National Park, Min Dat Township, Min Dat District, Chin State, Myanmar (21.38375°N, 98.89886°E, elevation 1787 m).

Paratypes. CAS 219993, adult male, same collection information as the holotype; CAS 233207, adult female, from Chun Kyone, Haka Township, Chin State, Myanmar (22.77231°N, 93.56411°E, elevation 1705 m) on July 15, 2003; CAS 233229, 233233, 233235, adult males; CAS 233232, 233234, adult females, all from Falam Township, Chin State, Myanmar (22.81439°N, 93.55752°E, elevation 1630 m), collected on July 18, 2003.

Etymology. The species name *iadina* is derived from Greek, which means "emerald" and refers to the bright green coloration of the new species.

Diagnosis. *Calotes iadina* **sp. nov.** can be diagnosed by a combination of the following morphological characters: (1) body size large, SVL 63.2–102.5 mm; (2) tail slender, long, TAL 293.9–367.9% SVL; (3) conical scales of two parallel ridges triangular shaped, relatively low, not in spine shape; (4) inferior row of conical scales 2–3 scale rows away from superior tympanum, TRD 14.8–28.8% TD; (5) mental larger than first pair of chin shields; (6) gular scale count 16–19, much larger than ventrals, strongly keeled, mucronate, each bearding a distinctively elongated tip on posterior end; (7) gular pouch feeble or absent, transverse gular fold absent; (8) shoulder fold present, covered with granular scales underneath; (9) nuchal crests relatively short, lanceolate shape, TNC 8.27–13.3% HL, dorsal crests moderately developed; (10) neck scales oriented posteriorly or posterosuperiorly; (11) axillary scales oriented vertically or near vertically; (12) dorsal body scales keeled, oriented posterosuperiorly, larger than ventrals; (13) middorsal crest scale count 39–43, (14) scale rows around midbody 48–53; (15) F4S 22–27, (16) T4S 27–33; (16) dorsal and ventral background coloration Yellow Green (Color 103) to Grass Green (Color 110) in normal condition, can change drastically to brownish to blackish under stress; (17) shoulder fold Pale Neutral Gray (Color 296) to Jet Black (Color 300); (18) white to Pale Pinkish Buff (Color 3) patches sometimes present on elbows, knees, and ankles, and same colored dorsolateral stripes sometimes present from neck to base of tail.

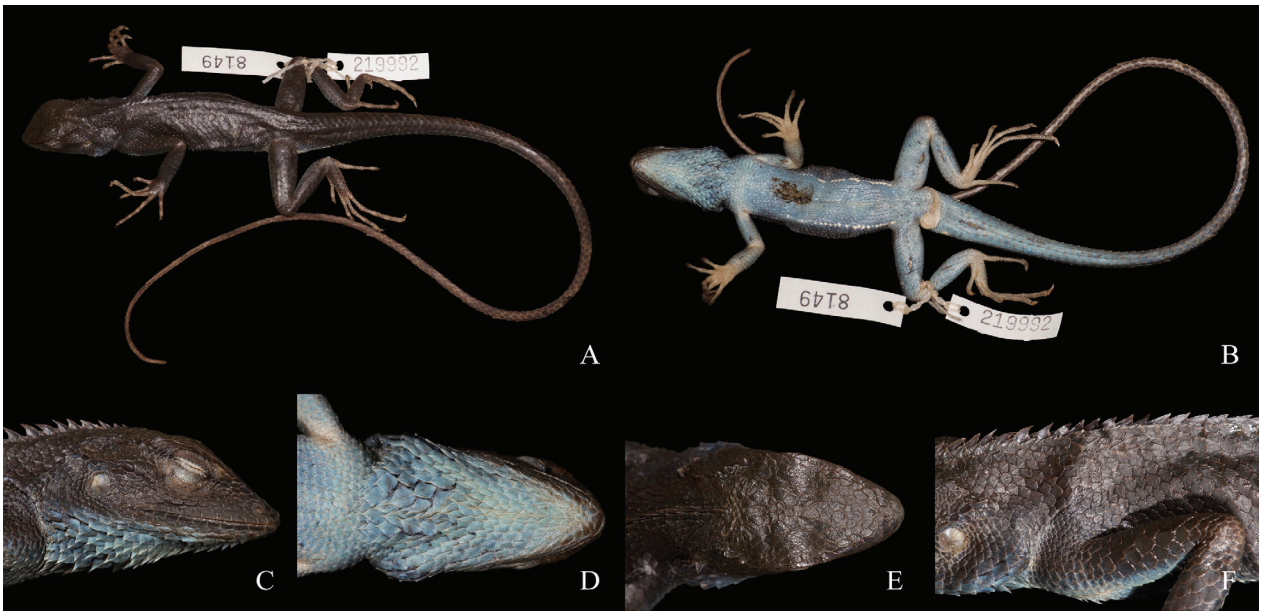

Figure 9. Holotype of *Calotes iadina* **sp. nov.** (CAS 219992), showing dorsal (**A**), ventral (**B**), lateral head (**C**), ventral head (**D**), dorsal head (**E**), and axillary region (**F**). Photos by Kai Wang.

Comparisons. The new species can be diagnosed from all congeners other than members of the *C. jerdoni* complex by having two parallel rows of conical or spinous scales on temporal region of the head (vs. absence). Within the *C. jerdoni* complex, *C. iadina* **sp. nov.** is most similar to *C. jerdoni*, but it differs from the latter by having vertical or near vertical orientation of axillary scales (vs. mostly oriented posteriorly or slightly upward, with an angle less than 60°; Fig. 4) and larger and fewer ventral scales (48–54 vs. 62–75). Moreover, the ANOVA analyses corroborated this statistical difference, recovering varying numbers of significantly different mean values between *C. iadina* **sp. nov.** and *C. jerdoni*, in which females of the new species differ from the females of *C. jerdoni* in having significantly different mean values head width (HD), interorbital distance (IOD), middorsal crest scale length (MD), tympanum diameter (TD), finger IV length (F4L), and orbital diameter (OD) (Appendix V). Males of *C. iadina* **sp. nov.** differ significantly from males of *C. jerdoni* in head length (HD), interorbital distance (IOD), tympanum diameter (TD), toe IV length (T4L), femur length (FEL), ventral scale count (VN), and orbital diameter (OD) (Appendix V).

For remaining species of the *C. jerdoni* complex, *C. iadina* **sp. nov.** differs from *C. yunnanensis* and *C. medogensis* by having larger and fewer gular scales along medial central axis (16–19 vs. 23–26 for *C. medogensis*, 20–23 for *C. yunnanensis*), presence of a distinct, elongated posterior tip on each gular scale (vs. absent or much shorter), larger and fewer ventral body scales (VEN 48–53 vs. 57–61 in *C. medogensis*, 54–62 in *C. yunnanensis*), and greatly overlapping supraciliaries (overlapping half of scale length vs. less than one third). Additionally, *C. iadina* **sp. nov.** differs from *C. yunnanensis* by having shorter nuchal crest scales (TNC 8.3–13.3% HL vs. 14.1–19.1%); from *C. medogensis* by having greatly overlapping supraciliaries (overlapping more than half of scale length vs. less than half); and from *C. maria* by having fewer scale rows between supratympanic ridge and superior edge of tympanae (1 or 2 rows vs. >3 rows), larger and fewer gular scales (16–19 vs. 27–31), much shorter nuchal crests (TNC 8.3–13.3% HL vs. >17.6%), the presence of shoulder fold (vs. absence), and the absence of spike-shaped scales on posterior end of the parallel ridges of the head (vs. presence). For the nomen dubium, *C. platyceps*, *C. iadina* **sp. nov.** differs by having more conical scales on the supratympanic ridge (6 or 7 vs. 8 or 9) and by the presence of a black stripe running through the eyes (vs. absence).

Description of holotype. Adult male, body size medium, SVL 84.5 mm, body not compressed, cross-section lachrymiform shaped; tail slender, long, TAL 364.0% SVL. Head narrow, somewhat elongate, HW 58.9% HL, HD 53.0% HL; jaw muscular, slightly swollen, HWJ 111.8% HW; snout length moderate, SEL 38.6% HL. Rostral rectangular, length four times height, bordering five small scales excluding supralabials, single scale away from nasal; nasal oval, in contact with first two supralabials; supralabials 11/10, 3–5 feebly keeled;

Figure 10. Type series of *Calotes iadina* **sp. nov.** in life, including the holotype (CAS 219992) (**A**) and paratypes [CAS 233207 (**B**), CAS 224511 (**C**), and CAS 219993 (**D**)]. Photos by Jens V. Vindum.

loreal slightly concave, loreal scales medium in size, all keeled, 5–7 scales away from orbit; eye surrounded by fine ciliary scales; suborbital scale rows 3/3, medial row much enlarged; canthal ridge distinct, canthus rostralis 10/11, supraciliaries overlapping about half scale length of consecutive ones. Two distinct ridges on temporal head, parallel anteriorly but joining posteriorly on squamosal region; superior ridge continuous from last canthal rostralis, consisting 7/6 conical scale that each bearing single lateral keel; inferior ridge starting post orbit, consisting 11/10 enlarged scales, anterior most two on each side smooth, convex, remaining ones conical, with posterior-most 2 largest and tallest, but none of them elongated into spikes; inferior ridges 1/2 scale rows away from tympana; region between two ridges slight concave; tympana exposed, oval, vertically oriented, TD 13.3% HL, OTD 22.0% HL; jaw scales enlarged, distinctively keeled, mucronate, imbricate. Dorsal head scales weakly keeled, heterogeneous in size and shape; enlarged scales arranged in Y-shape, single scales posterior to rostral along longitudinal midline, all about equal size; 14 scales transversely across dorsal head between supraciliary at widest point; parietal scale enlarged, narrow, elongated, parietal eye distinct; scales posterolateral of parietal bearing oblique keels.

Mental triangular, separating and much larger than first pair of chin shields; chin shield 8/7, first three on each side in direct contact with infralabials, remaining ones separated by single, small scale-row; first four chin shields smooth, remaining one each bearing single indistinct lateral keel; remaining gular scales all distinctively keeled, imbricate, mucronate with long tips, gradually increasing in size posteromedially, gular scales 16 along central-medial line.

Dorsal body scales feebly keeled, more distinct anteriorly on neck and inferiorly close to ventrolateral flank, mostly homogeneous in size; scales on neck oriented horizontally backward or obliquely upward at less than 45°; axillary scales smaller, oriented near vertically, which then gradually change to a more oblique orientation superiorly and posteriorly; shoulder fold present, distinct, with granular fine scales underneath; flank scales large, with minimal lateral keel on posterior tip only, imbricate in regular oblique rows, 45 scale rows at mid body. Crest distinct, nuchal crest not significantly differentiated from dorsal crests, lanceolate shaped, relatively short, TNC 11.9% HL; middorsal crest scale 41, gradually reducing height posteriorly, crest scale height equal width from anterior one third of body, remaining dorsal crests longer than height. Dorsal scales on limbs mostly homogeneous in size and shape, smooth or feebly keeled, keel status slightly more distinct proximally on lower appendages. Tail swollen at base, feebly keeled on anterior one sixth of length, gradually increasing in keel status posteriorly and forming carinate rows.

Ventral body scales smaller than gulars and dorsals, distinctively keeled, mucronate, imbricate, forming carinate rows; ventral scale row 51; F4S 27/25, T4S 32/33; ventral limb scales more distinctively keeled; ventral tail scales more distinctively keeled, carinate at base.

Coloration. In life, background coloration is light grass green. Distinct black radial stripes are present around eyes, forming a transverse oriented Y-shape across eyes, with its opening facing posteriorly. The shoulder fold is black. Numerous indistinct, black, oblique transverse stripes are present on flank. The gular and ventral body are lighter and more yellowish. Two parallel rows of single white scales are present on ventrolateral body between axillary and groin. Under preservation, the dorsal background green body coloration turns into dark bluish gray, and the ventral color turns into light blue.

Variation. Morphometric and pholidosis variation are summarized in Table 4. Additionally, all paratypes have more distinctly keeled scales on the dorsal surface of the limbs than the holotype. Two preserved female paratypes (CAS 233232 and 233234) possess light-gray dorsolateral stripes, which extend from the neck to the base of tail. Some individuals also have indistinct oblique transverse stripes (CAS 233233 and 233234).

Natural history and conservation. Based on collection notes, specimens were found along a road during morning hours, although the species is likely to be arboreal. Some of the females were gravid, suggesting that breeding occurs during July. Currently, the species is only known from western Myanmar along the Chin Hills, and no imminent conservation threat is known. The species is known to be capable of changing its ground color, from blackish brown to its original green (Fig. 9). Given the lack of data on habitat quality and population trend, we propose to list the new species as Data Deficient (DD) for its IUCN assessment.

Calotes yunnanensis Annandale, 1905

Figures 4, 11, 12, Table 3, Appendix II

Chresonymy.

Calotes maria – Anderson (1879: 806)

Calotes jerdoni – Pope (1935: 468–469), Smith (1935: 194–195), Zhao and Adler (1993: 188), Zhao and Yang (1997: 156–157), Zhao et al. (1999: 90–91), Yang and Rao (2008: 189), Wang et al. (2020: appendix), Wang et al. (2022: appendix)

Holotype. ZSI 6571, adult female from Teng-yue, western Yunnan, China.

Remarks on the type locality, gender, and measurements of holotype. Most studies have considered Teng-yue as interchangeable with the modern Tengchong County in Yunnan Province (Zhao and Adler, 1993), including the museum label of the holotype at ZSI. Although Teng-yue includes the modern Tengchong County, they are not interchangeable: Teng-yue was the administrative unit of the Qing Dynasty and encompassed a much larger area west of the Gaoligong Mountains, which also includes modern-day Dehong Prefecture. Therefore, the type locality of the species should be revised as both mod-

ern-day Dehong Prefecture and Baoshan (which include Tengchong County).

Annandale (1905) noted that the holotype of *C. yunnanensis* is a male. However, our examination shows it to be a female (e.g., no distinct bulge at base of tail as in male specimens such as KIZ 014148, 029968, and 039747). Also, in the original description, Annandale (1905) measured the head length of the holotype as 34 mm and body length as 65 mm, which differs greatly from our measurement of head length (27.2 mm) and SVL (94.8 mm). As Annandale (1905) did not specify his measurement method, these differences could be explained by different measurement methods.

Additional examined specimens. Topotypes: KIZ 014148, 029968, 039747, adult males; KIZ 015993, 014146, 014147, 030060, 50692, 034358, adult females; all from Yingjiang County, Dehong Prefecture, Yunnan, China. CAS 224511, adult male, from Nagmung Township, Putao, Kachin State, Myanmar (27.440861°N, 97.8950278°E, 573 m); CAS 221514, adult female, from Naung Mon Township, Putao, Kachin State, Myanmar (27.44122°N, 97.91875°E, 535 m); CAS 221551, adult female, from Machanbaw Township, Putao District, Kachin State, Myanmar (27.28994°N, 97.858472°E, 708 m); CAS 245278, adult female from Lahe township, Khandi District, Sagaing Division, Myanmar (26.324194°N, 95.44875°E, 900 m); CAS 245364, adult female, from Laung Nguk Village, Lahe Township, Sagaing Division, Myanmar (26.1590278°N, 95.529167°E, 833m).

Diagnosis. *Calotes yunnanensis* is diagnosed from congeners by a combination of the following characters: (1) body size large, SVL 73–120 mm; (2) tail slender, long, TAL 311.8–353.7% SVL; (3) conical scales forming two parallel ridges from posterior eye to temporal head, posterior most 3–5 scales of superior ridge distinctively differentiated but relatively low; (4) inferior ridge of conical scales 2–3 scale-rows away from superior tympanum, TRD 38.4–52.5% TD; (5) dorsal head scales posterolateral to parietal bearing oblique or lateral keels; (6) mental larger or about equal to first pair of chin shields; (7) gular scale count 21–25 along central-medial line, equal or larger than ventrals, strongly keeled, slightly mucronate, keel extending across entirety of each scale and elongated on posterior end into very short tips; (8) gular pouch present in life, weakly developed, but absent after preservation; (9) transverse gular fold absent; (10) shoulder fold present, short, covered with granular scales underneath; (11) nuchal crests long, lanceolate shape, dorsal crests moderately developed, TNC 14.1–21.2% HL; (12) neck scales and dorsal body scales weekly keeled, oriented upwards and backwards, larger than ventrals; (14) axillary scales oriented near vertically; (13) middorsal crest scale count 38–45, (14) scale rows around midbody 51–60; (15) ventral scale count 54–68; (16) F4S 26–29, T4S 31–34; (17) dorsal and ventral background coloration Yellow Green (Color 103) to Grass Green (Color 110) in normal condition, can change drastically to dark brown to blackish under stress; (18) shoulder fold Pale Neutral Gray (Color 296) to Brick Red (Color 36); (19) white to Pale Pinkish Buff (Color 3) patches present on elbows, knees, and ankles; and (20) Pale Pinkish Buff (Color 3) dorsolateral stripes from neck to basal tail present in some individuals.

Comparisons. *Calotes yunnanensis* can be diagnosed from all congeners other than members of the *C. jerdoni* complex by having two parallel rows of conical or spinous scales on temporal region of the head (vs. absence) and by the absence of post orbital spikes (vs. presence).

For members of the *C. jerdoni* complex, *C. yunnanensis* was confused with *C. maria* and *C. jerdoni*, but it can be diagnosed from *C. maria* by the presence of a shoulder fold (vs. absence), a shorter distance between supratympanic ridge and tympanum (1–3 scales away vs. four or five scales); and from *C. jerdoni* by having a different

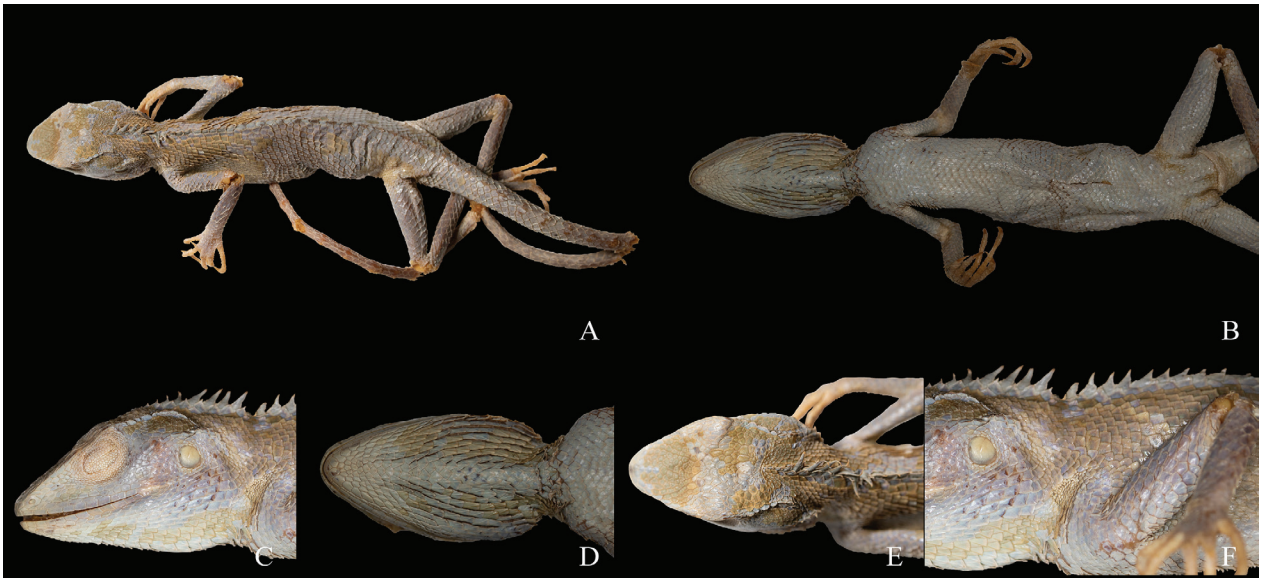

Figure 11. Holotype of *Calotes yunnanensis* (ZSI 6571), showing dorsal (**A**), ventral (**B**), lateral head (**C**), ventral head (**D**), dorsal head (**E**), and axillary region (**F**). Photos by V. Deepak and Abhijit Das.

shape of gular scales (heterogeneous in size, smaller in posteromedial region, without elongated tips or tips very short vs. homogeneous in size, with distinct, elongated tips), smaller gular scales and higher scale count (22–25 vs. 16–19), and by having longer nuchal crest scales (TNC 14.1–19.1% HL vs. 8.1–13.2%).

Morphologically, *C. yunnanensis* is most similar to *C. medogensis*, but it differs from the latter by having obliquely or longitudinally oriented keels on scales posterolateral to the parietal (vs. transversely oriented keels), larger mental scale relative to first pair of chin shields (vs. smaller), more distinctly keeled gular scales, particularly on posterolateral region (keel extending across the entirety of each scale vs. only extending across posterior half or less), and by the presence of white dorsolateral stripes on some individuals (vs. always absent) (Fig. 4).

Description of holotype. Adult female, body size medium, SVL 94.8 mm, body not dorsally compressed, cross-section triangular shaped; tail slender, broken. Head somewhat elongate, HW 63.6% HL, HD 60.4 % HL; jaw not distinctively swollen; snout length moderate, SEL 44.4% HL. Rostral rectangular, length four times height, two scales away from nasal; nasal oval, separated from first supralabials by single scale; supralabials 11/10, all smooth; loreal region slightly concave, loreal scales medium in size, all keeled, 6 scales away from orbit; eye surrounded by fine ciliary scales; suborbital scale rows 3/3, medial row much enlarged; canthal ridge distinct, canthus rostralis 10/10, supraciliaries overlapping about one third length. Two distinct ridges on temporal head, parallel anteriorly but joining posteriorly on squamosal region; anterior ridge continuous from last canthal rostralis, consisting 10/10 conical scale that each bearing single lateral keel; inferior ridge starting post orbit, consisting 9/10 enlarged scales, each bearing single lateral keel; inferior ridges 3 scale rows away from tympana; region between two ridges slight concave; tympana exposed, oval, vertically oriented, TD 12.7% HL; jaw scales enlarged, moderately keeled, slightly mucronate, imbricate. Dorsal head scales weakly keeled, heterogeneous in size and shape; slightly enlarged scales arranged in Y-shape, single scales posterior to rostral along longitudinal midline, all about equal size; 16 scales transversely across dorsal head between supraciliary at widest point; parietal scale enlarged, rectangular, parietal eye distinct; scales posterolateral of parietal bearing oblique keels.

Mental triangular, smaller than and separating first pair of chin shields; chin shields 6/7, first two on each side in direct contact with infralabials, remaining ones separated by one or two small scale-row; first four chin shields smooth, remaining one each bearing single weak lateral keel; remaining gular scales all distinctively keeled, imbricate, mucronate, some bearing single short tip, gradually increasing in size posteromedially, gular scale 23.

Dorsal body scales feebly keeled, mostly homogeneous in size; scales on neck oriented obliquely upward at about 45°; axillary scales smaller, oriented near vertically, which then gradually changing to a more oblique orientation superiorly and posteriorly; shoulder fold present, distinct, with granular fine scales underneath; flank scales large, mostly smooth, some with minimal lateral keel on posterior tip only, imbricate in regular oblique rows, 56 scale

Figure 12. Topotypic individuals of *Calotes yunnanensis* in life, including KIZ 014146 (**A**), KIZ 014148 (**B**), KIZ 014147 (**C**), and a non-vouchered individual (**D**). Photos by Yu-Fan Wang and Zheng-Pan Duan.

rows at mid body. Crest distinct, nuchal crest not significantly differentiated from adjacent dorsal crests, lanceolate shaped, relatively long; middorsal crest scale 45, gradually reducing height posteriorly. Dorsal scales on limbs mostly homogeneous in size and shape, smooth or feebly keeled, keel status slightly more distinct proximally on lower appendages. Tail not swollen at base, broken in four sections, scales feebly keeled on anterior part, gradually increasing in keel status posteriorly and forming carinate rows.

Ventral body scales smaller than gular and dorsals, distinctively keeled, mucronate, imbricate, forming carinate rows; ventral scale row 58; ventral scales of limbs more distinctively keeled. Limbs slender, partially broken at elbow and knee joints.

Coloration. The holotype is nearly uniform light-gray, with the temporal region slightly darker, and the ventral surface paler. For newly collected specimens, the coloration in life varies drastically based on the mood and status of the lizards. The background coloration of dorsal and lateral surfaces ranges from Cinnamon (Color 255) to bright Pistachio (Color 102). Some individuals possess Light Buff (Color 2) dorsolateral stripes from the neck to the anterior one third of tail, some Light Buff (Color 2) or Clay Color (Color 18) oblique stripes on dorsum, and others are uniformly colored with no ornamentation patterns. All individuals possess Light Buff (Color 2) patches on limb joints, either on elbows, knees, ankles, or any combination of thereof. The palate and buccal mucosa are Jet Black (Color 300), but the gums and the tongue are Pink (Color 242).

Natural history, distribution, and conservation. Currently, *C. yunnanensis* has been recorded from the southwestern Yunnan Province of China and Sagaing and Kachin States of Myanmar. It likely inhabits northern Shan State in Myanmar as well. Anderson (1879) speculated that *C. yunnanensis* (identified as *C. maria* at the time) is less arboreal than *C. versicolor* and *C. emma*, because the collecting site was mostly deforested. However, based on our field observations, we found this is not true: *C. yunnanensis* is highly arboreal, and individuals were found inhabiting well-forested tropical and subtropical regions in Southwest Yunnan.

In China, although the habitat of *C. yunnanensis* is well-protected by nature reserves, it has very restricted range, and has been targeted by domestic illegal pet traders (yingjiang.gov.cn, 2019). On the other hand, globally, *C. yunnanensis* has a considerable distribution range that consists of well-preserved habitats. Therefore, we assess the species as Near Threatened (NT) for China's domestic Red List Assessment, and as Least Concern (LC) globally based on IUCN criteria.

Identification Key

To facilitate future taxonomic research, we update the diagnostic key and distribution of the recognized species of the *C. jerdoni* complex based on the results of this paper:

1 One or two parallel ridges of conical or distinctively keeled and raised scales posterior to orbit; background coloration bright green in relaxed state in life..... ***C. jerdoni* complex**

1a No shoulder fold; tympanum 4 or 5 scale-rows away from supratympanic ridge; posterior-most 3 or 4 scales of parallel ridges distinctively elongated into spikes, longest one about same length as longest nuchal crest; nuchal crest long, narrow, TNC 17.6–24.0% HL; gular scales small, 27–31..... ***C. maria*** (Meghalaya, India)

1b Shoulder fold present, composed of small granular scales; tympanum separated by only 1 or 2 scale rows from supratympanic ridge; posterior-most 3 or 4 scales of parallel ridges not distinctively elongated into spikes; nuchal crest mostly shorter, spikes much wider at base 2

2a Gular scales larger, more homogeneous, ≤19, with distinctively elongated tips, particularly along medial longitudinal axes.....3

2b Gular scales smaller, more heterogeneous, ≥20, without elongated tips or tips very short 4

3a Axillary scales pointed posteriorly or posterosuperiorly at angle less than 60°; ventral scales smaller, ≥62; tail relatively shorter (average TAL/SVL 305.5% in males, 293.6% in females)..... ***C. jerdoni*** (Assam, Nagaland, and Meghalaya, India; possibly China [Southern Xizang Autonomous Region])

3b Axillary scales pointed vertically upward or posterosuperiorly at angle larger than 60°; ventral scales larger, ≤54; tail relatively longer (average TAL/SVL 347.6% in males, 313.6% in females)..... ***C. iadina* sp. nov.** (Chin State, Myanmar)

4a Nuchal crest longer, TNC 13.1–21.2% HL; keels of dorsal head scales posterolateral to parietal scale obliquely or longitudinally oriented; mental larger or approximately equal in size to first pair of chin shields; keels of posterolateral gular scales nearly extending across the entire length of scale; some individuals bear distinct dorsolateral stripes on dorsum ..... ***C. yunnanensis*** (Kachin State and Shan State, Myanmar; Yunnan Province, China)

4b. Nuchal crest short, TNC 5.2–15.7% HL; keels of dorsal head scales posterolateral to parietal scale transversely oriented; mental smaller than first pair of chin shields; keels of posterolateral gular scales extending less than half of scale length; no dorsolateral stripes on dorsum..... ***C. medogensis*** (Xizang Autonomous Region, China; northeast India)

Discussion

Distribution of *Calotes* in Myanmar

While recent studies have improved our understanding of the diversity and distribution of *Calotes* in Myanmar (Vindum et al. 2003; Zug et al. 2006; Gowande et al. 2021; Wagner et al. 2021), much remains unresolved about *Calotes* populations in that country. Previously, *C. jerdoni* was the only member of the *C. jerdoni* complex recorded from Myanmar (Vindum et al. 2003; Zug et al. 2006). Based on our taxonomic revision, we confirm there are two species of the complex in Myanmar: *C. iadina* **sp. nov.** and *C. yunnanensis*. Specifically, *C. iadina* **sp. nov.** is from the Chin Hills in central western Myanmar and *C. yunnanensis* is from both the western edge of the Shan Plateau in eastern Myanmar and northern montane region in Putao. Detailed surveys are needed in the future to obtain a better understanding of the fine scale distribution, conservation status, and general natural history of these two species in Myanmar.

For the recent revision of the *C. mystaceus* complex across Indochina, we follow Wang et al. (2022) and do not recognize the new species described by Wagner et al. (2021). On one hand, the mitochondrial genealogy by Wagner et al. (2021) failed to resolve the relationships among clades within the *C. mystaceus* complex. While on the other hand, the proposed morphological diagnosis of coloration patterns by Wagner et al. (2021) is not only highly variable among individuals, but colors are variable within the same individual based on its mood and body temperature. As their morphological "diagnoses" cannot consistently differentiate their "species", and given the lack of meaningful results from their morphometric analyses, we do not agree with their taxonomic treatment. Future studies with more stringent integrative methods are needed to further test the current taxonomic hypotheses within the *C. mystaceus* complex in Southeast Asia.

Similar to Zug et al. (2006), our molecular phylogeny shows that the *C.* cf. *emma* from southwestern Myanmar (CAS 223060, Genbank accession number DQ289460) is sister to *C. chincollium* and paraphyletic with respect to *C. emma* from eastern Indochina. Given its minimal genetic divergence from *C. chincollium*, we suggest it is a likely misidentification of *C. chincollium*, and the range of *C. chincollium* extends further south along the Chin Hills. Future studies should always verify the taxonomic identification of the genetic data from Genbank.

With the exclusion of the questionable species of the *C. mystaceus* complex (i.e., *C. geissleri*, *C. goetzi*, and *C. vindumbarbatus*), there are eight species of *Calotes* currently recorded in Myanmar (Zug et al. 2006; Platt et al. 2018; Uetz et al. 2022; present study), including *C. chincollium*, *C. emma*, *C. irawadi*, *C. htunwini*, *C. mystaceus*, *C. iadina* **sp. nov.**, and *C. yunnanensis*.

Paucity of data on recognized species and questionable records of "*Calotes jerdoni*" across the Pan-Himalaya

Even after this revision of the *Calotes jerdoni* complex, many recognized species still lack basic data on their phylogenetic position and natural history (e.g., *C. maria*). Additionally, multiple questionable records of "*C. jerdoni*" still exist across the Pan-Himalaya, particularly in China, northeast India, and Bhutan. In China, "*C. jerdoni*" has been recorded from two provinces, namely Yunnan and Xizang Autonomous Region (Zhao et al. 1999; Che et al. 2020; Wang et al. 2022). For Yunnan Province, "*C. jerdoni*" has been reported from Teng-yue in the southwest and Xishuangbanna in the south (Zhao et al. 1999; Yang and Rao 2008; Wang et al. 2022). With our data, we confirm that the population from Teng-yue in southwestern Yunnan should be replaced by the newly resurrected *C. yunnanensis*. On the other hand, the voucher record from Xishuangbanna in southern Yunnan (CIB 605281) (Zhao et al. 1999) disagrees with the diagnosis of *C. jerdoni* complex by lacking the parallel ridges of conical scales on the head (CIB 625281; Fig. 13), and it matches the morphological diagnosis of *C. mystaceus* complex (e.g., relatively shorter tail, presence of white lip-stripe). Therefore, all records of *C. jerdoni* from Yunnan Province of China should be removed and updated.

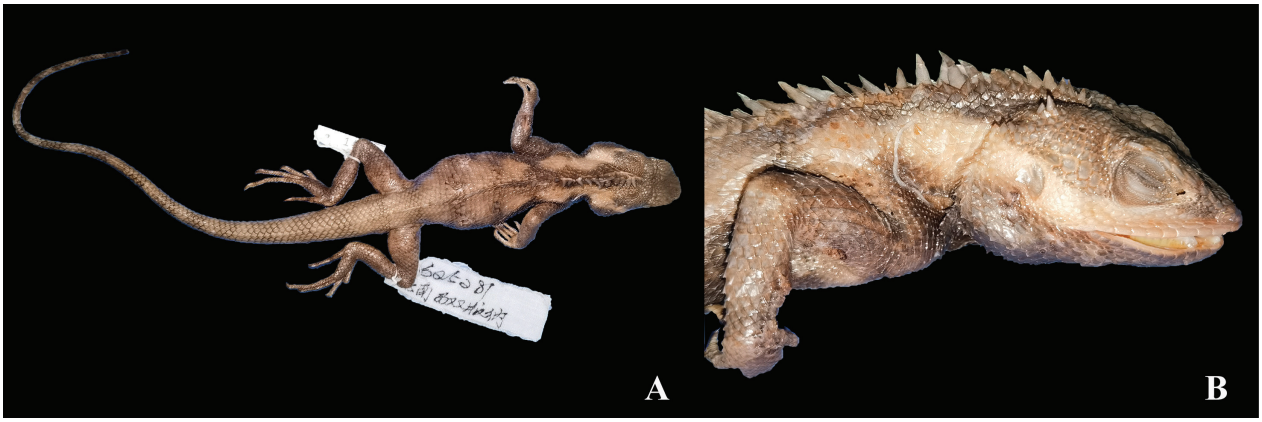

Figure 13. Voucher specimen of the previous record of "*Calotes jerdoni*" from Xishuangbanna, southern Yunnan Province (CIB 605281), which is a mis-identified *C. mystaceus* sensu lato. **A** dorsal view; **B** lateral head view. Photos by Ke Jiang.

For the Xizang Autonomous Region, "*C. jerdoni*" has been reported from two localities, namely from the Nepal-China border region in Zhangmu (Zhao and Adler 1993) and from Medog County (Che et al. 2020). While the record from Zhangmu has been shown to represent a misidentified *Japalura tricarinata* (Schleich and Kästle 2002; Wang et al. 2018; Uetz et al. 2023), the record from the India-China border region in Medog has been overlooked by most authors (Hu et al. 1987; Zhao et al. 1999; Li et al. 2010; Uetz et al. 2023). This overlooked Xizang record of "*C. jerdoni*" is allopatric to the true *C. jerdoni* in the low-elevation Assam Plains (Fig. 1). Based on photographs (media code bm330, Kamdar et al. 2022), individuals of these allopatric populations disagree with our revised morphological diagnosis of true *C. jerdoni*, specifically differing in the shape of gular scales (only slightly mucronate with very short tips vs. distinctively mucronate with long tips for true *C. jerdoni*). Therefore, the only remaining Chinese population of "*C. jerdoni*" from Southern Xizang Autonomous Region may also be a misidentification of a yet undescribed species, and the true *C. jerdoni* may not be found in China. Without voucher specimens, we tentatively retain the Xizang record of *C. jerdoni*, pending future evidence.

Even in the proximity of the type locality of *C. jerdoni* in northeast India, additional cryptic diversity may also exist (Fig. 1). For the previous record of "*C. jerdoni*" in Bhutan, based on published photographs (Tshewang and Letro 2018; Bhutan Biodiversity Portal 2023), individuals from Bhutan only have a single row of conical scales between the orbit and the tympanum, which is different from true *C. jerdoni* that has two parallel rows. It is likely that the Bhutan questionable populations represent additional cryptic species of the complex in the East Himalayas and warrant taxonomic descriptions. Future studies with wider sampling and genetic data are needed to fully understand the taxonomy and distribution of the *C. jerdoni* complex across the East Himalayas.

Acknowledgements

Field surveys and collections of specimens follow relevant regulations in China and India. We thank Dr Wolfgang Denzer for his constructive feedback on the manuscript; Tongbiguan Provincial Nature Reserve in China for their permission and supports in field surveys; Zheng-Pan Duan, Ke Jiang, Ben-Fu Miao, Yu-Fan Wang, and Li-Yan Wang for their assistance in the field in China, and Vivek Sarkar in the field in India. This project was supported by grants from the National Key R&D Program of China (2022YFC2602500), Science and Technology Basic Resources Investigation Program of China (2021FY100200),the Second Tibetan Plateau Scientific Expedition and Research Program (STEP) (2019QZKK0501), China's Biodiversity Observation Network (Sino-BON), and Yunnan Revitalization Talent Support Program Yunling Scholar Project to JC; Yunnan Forestry and Grassland Administration (2022GF258D-10), Survey of Wildlife Resources in Key Areas of Tibet, China (ZL202203601), the Animal Branch of the Germplasm Bank of Wild Species, Chinese Academy of Sciences (the Large Research Infrastructure Funding), CAS Special Research Assistant (SRA) Program, and Yunnan Revitalization Talent Support Program Young Talent Project to WK; and the Humboldt fellowship hosted by Uwe Fritz at the Senckenberg Dresden to VD. VD thanks Patrick Campbell and David Gower for their support while studying the NHM, London collections. AD thanks SERB-DST (CRG/2018/000790) for financial support and Director, WII for institutional support. VD and AD thanks Kaushik Deuti, Prabat Bag, Sujoy Raha, students, and other staff at ZSIK for their curatorial support.

References

Ananjeva NB, Guo X, Wang Y (2011) Taxonomic diversity of agamid lizards (Reptilia, Sauria, Acrodonta, Agamidae) from China: A comparative analysis. Asian Herpetological Research 2: 117–128. https://doi.org/10.3724/SP.J.1245.2011.00117

Anderson J (1879 "1878") Reptilia and amphibia. In: Anderson J (Ed.) Anatomical and Zoological Researches: Comprising an account of the zoological results of the two expeditions to western Yunnan in 1868 and 1875; and a monograph of the two cetacean genera *Platanista* and *Orcella*, Volume I. Bernard Quaritch, London, 985 pp.

Annandale N (1905) Contributions to oriental herpetology, supplement II: Notes on oriental lizards in the Indian Museum, with a list of the species recorded from British India and Ceylon. Proceedings of the Asiatic Society of Bengal 2: 81–93.

Bhutan Biodiversity Portal (2023) Available from URL: https://biodiversity.bt/observation/show/62644 [accessed 11 June 2023]

Blyth E (1852) Report of curator, zoological department. Journal of the Asiatic Society of Bengal 21: 341–358.

Blyth E (1853) Report of the curator, zoological department. Journal of the Asiatic Society of Bengal: 411–413.

Boruah B, Narayanan S, Deepak V, Das A (2022) Morphological and molecular differences in two closely related *Calotes* Cuvier, 1817 (Squamata: Agamidae: Draconinae) with the first record of *C. medogensis* Zhao and Li, 1984 from India. Zootaxa 5219: 433–455. https://doi.org/10.11646/zootaxa.5219.5.3

Boulenger GA (1885) Catalogue of the Lizards in the British Museum (Natural History), Volume I: Geckonidae, Eublepharidae, Uroplatidae, Pygopodidae, Agamidae. British Museum (Natural History), London, 436 pp.

Boulenger GA (1890) The Fauna of British India, Including Ceylon and Burma. Reptilia and Batrachia. Taylor & Francis, London, 541 pp.

Chan KO, Grismer LL (2022) GroupStruct: An R package for allometric size correction. Zootaxa 5124: 471–482. https://doi.org/10.11646/zootaxa.5124.4.4.

Che J, Jiang K, Yan F, Zhang YP (2020) Amphibians and Reptiles in Tibet—Diversity and Evolution. Science Press, Beijing, 803 pp. [in Chinese].

Darriba D, Taboada GL, Doallo R, Posada D (2012) jModelTest 2: More models, new heuristics and parallel computing. Nature Methods 9: 772. https://doi.org/10.1038/nmeth.2109

Deepak V, Vyas R, Giri V, Karanth K (2015) A taxonomic mystery for more than 180 years: The identity and systematic position of *Brachysaura minor* (Hardwicke & Gray, 1827). Vertebrate Zoology 65: 371–381. https://doi.org/10.3897/vz.65.e31528

Dever JA, Fuiten AM, Konu Ö, Wilkinson JA (2012) Cryptic torrent frogs of Myanmar: An examination of the *Amolops marmoratus* species complex with the resurrection of *Amolops afghanus* and the identification of a new species. Copeia 2012: 57–76. https://doi.org/10.1643/CH-10-180

Giri VB, Chaitanya R, Mahony S, Lalrounga S, Lalrinchhana C, Das A, Sarkar V, Karanth P, Deepak V (2019) On the systematic status of

the genus *Oriocalotes* Günther, 1864 (Squamata: Agamidae: Draconinae) with the description of a new species from Mizoram state, Northeast India. Zootaxa 4638: 451–484. https://doi.org/10.11646/zootaxa.4638.4.1

Gowande G, Mishra A, Mirza ZA (2016) Neotype designation for *Calotes versicolor* Daudin, 1802 (Sauria: Agamidae) with notes on its systematics. Zootaxa 4126: 271–279. http://doi.org/10.11646/zootaxa.4126.2.7

Gowande G, Pal S, Jablonski D, Masroor R, Phansalkar PU, Dsouza P, Jayarajan A Shanker K (2021) Molecular phylogenetics and taxonomic reassessment of the widespread agamid lizard *Calotes versicolor* (Daudin, 1802) (Squamata, Agamidae) across South Asia. Vertebrate Zoology 71: 669–696. http://doi.org/10.3897/vz.71.e62787

Gray JE (1845) Catalogue of the specimens of lizards in the collection of the British Museum. Trustees of die British Museum/Edward Newman, London, 289 pp.

Guindon S, Gascuel O (2003) A simple, fast, and accurate algorithm to estimate large phylogenies by maximum likelihood. Systematic Biology 52: 696–704. https://doi.org/10.1080/10635150390235520

Günther A (1870) Descriptions of a new Indian lizard of the genus *Calotes*. Proceedings of the Zoological Society of London 1870: 778–779.

Hallermann J (2000) A new species of *Calotes* from the Moluccas (Indonesia), with notes on the biogeography of the genus (Sauria: Agamidae). Bonner Zoologische Beiträge 49: 155–163.

Hartmann T, Geissler P, Poyarkov NA Jr, Ihlow F, Galoyan EA, Roedder D, Böhme W (2013) A new species of the genus *Calotes* Cuvier, 1817 (Squamata: Agamidae) from southern Vietnam. Zootaxa 3599: 246–260. http://dx.doi.org/10.11646/zootaxa.3599.3.3

Hillis DM, Bull JJ (1993) An empirical test of bootstrapping as a method for assessing confidence in phylogenetic analysis. Systematic Biology 42: 182–192. https://doi.org/10.2307/2992540

Hu S, Zhao EM (1987) Amphibians and Reptiles of Tibet. Science Press, Beijing, 153 pp.

Husson F, Josse J, Le S, Mazet J (2017) FactoMine R: Exploratory data analysis and data mining. R package, version 1.36.

ICZN [International Commission on Zoological Nomenclature] (1999) International Code of Zoological Nomenclature. 4th Edition. The International Trust for Zoological Nomenclature, London, 306 pp.

Jerdon TC (1853) Catalogue of the Reptiles inhabiting the Peninsula of India. Part 1. Journal of the Asiatic Society of Bengal 22: 462–479.

Kamdar A, Jangid A, Roy P, Kunte K (2022) Reptiles of India, v. 1.26. Indian Foundation for Butterflies. https://www.indianreptiles.org/ifoundbutterflies

Kassambara A, Mundt F (2017) Factoextra: Extract and visualize the result of multivariate data analyses. R package, version 1.0.5.999.

Köhler G (2012) Color Catalogue for field biologists. Herpeton, Offenbach, 49 pp.

Li PP, Zhao EM, Dong BJ (2010) Amphibians and Reptiles of Tibet. Science Press, Beijing, 249 pp. [In Chinese].

Lleonart J, Salat J, Torres GJ (2000) Removing allometric effects of body size in morphological analysis. Journal of Theoretical Biology 205: 85–93. https://doi.org/10.1006/jtbi.2000.2043

Manthey U (2010) Agamid Lizards of Southeastern Asia. Draconinae 1– Leiolepidinae (Terralog 7b). Edition Chimaira, Frankfurt, 168 pp.

Marshall DC (2010) Cryptic failure of partitioned Bayesian phylogenetic analyses: Lost in the land of long trees. Systematic Biology 59: 108–117. https://doi.org/10.1093/sysbio/syp080

McCoy MW, Bolker BM, Osenberg CW, Miner BG, Vonesh JR (2006) Size correction: Comparing morphological traits among populations and environments. Oecologia 148: 547–554. https://doi.org/10.1007/s00442-006-0403-6

Oksanen J, Blanchet FG, Friendly M, Kindt R, Legendre P, McGlinn D, Minchin PR, O'Hara RB, Simpson GL, Solymos P, Henry M, Stevens H, Szoecs E, Wagner H (2020) Package Vegan: Community ecology package version 2.3. Available from https://cran.r-project.org, https://github.com/vegandevs/vegan

Pagès J (2015) Multiple Factor Analysis by Example Using R. CRC Press, New York, 272 pp.

Pal S, Vijayakumar SP, Shanker K, Jayarajan A, Deepak V (2018) A systematic revision of *Calotes* Cuvier, 1817 (Squamata: Agamidae) from the Western Ghats adds two genera and reveals two new species. Zootaxa 4482: 401–450. https://doi.org/10.11646/zootaxa.4482.3.1

Platt SG, Zug GR, Platt K, Ko KW, Myo KM, Soe MM, Lwin T, Win MM, Aung SHN, Kyaw NW, Thu H, Wint KTZW, Dijk PP, Horne BD, Rainwater TR (2018) Field records of turtles, snakes, and lizards in Myanmar (2009–2017) with natural history observations and notes on folk herpetological knowledge. Natural History Bulletin of the Siam Society 67: 67–114.

Pope CH (1935) The Reptiles of China, Turtles, Crocodilians, Snakes, Lizards, Natural History of Central Asia 10. American Museum of Natural History, New York, NY, 604 pp.

R Core Team (2018) R: A language and environment for statistical computing. R Foundation for Statistical Computing, Vienna. Available from: http://www.R-project.org.

Rambaut A, Drummond AJ, Xie D, Baele G, Suchard MA (2018) Posterior summarization in Bayesian phylogenetics using Tracer 1.7. Systematic Biology 67: 901–904. https://doi.org/10.1093/sysbio/syy032

Reist JD (1986) An empirical evaluation of coefficients used in residual and allometric adjustment of size covariation. Canadian Journal of Zoology 64: 1363–1368. https://doi.org/10.1139/z86-203

Ronquist F, Teslenko M, Van Der Mark P, Ayres DL, Darling A, Höhna S, Larget B, Liu L, Suchard MA, Huelsenbeck JP (2012) MrBayes 3.2: Efficient Bayesian phylogenetic inference and model choice across a large model space. Systematic Biology 61: 539–542. https://doi.org/10.1093/sysbio/sys029

Schleich HH, Kästle W (2002) Amphibians and Reptiles of Nepal. Koeltz Scientific Books, Koenigstein, 1211 pp.

Schulte JA, Vindum JV, Win H, Thin T, Lwin KS, Shein AK (2022) Phylogenetic relationships of the genus *Ptyctolaemus* (Squamata: Agamidae), with a description of a new species from the Chin Hills of western Myanmar. Proceedings California Academy of Sciences 55: 222–247.

Skalski JR, Richins SM, Townsend RL (2018) A statistical test and sample six recommendations for comparing community composition following PCA. PloS ONE 13: e0206003. https://doi.org/10.1371/journal.pone.0206033

Smith MA (1935) The fauna of British India, including Ceylon and Burma. Reptiles and Amphibia, Vol. II. Sauria. Taylor and Francis, London, 440 pp.

Stamatakis A (2014) RAxML version 8: A tool for phylogenetic analysis and post-analysis of large phylogenies. Bioinformatics 30: 1312–1313. https://doi.org/10.1093/bioinformatics/btu033

Stamatakis A, Hoover P, Rougemont J (2008) A rapid bootstrap algorithm for the RAxML web servers. Systematic Biology 57: 758–771. https://doi.org/10.1080/10635150802429642

Swofford DL, Sullivan J (2003) Phylogeny inference based on parsimony and other methods using PAUP*. In: Bottu G (Ed.) The Phyloge-

netic Handbook: A Practical Approach to DNA and Protein Phylogeny. Cambridge University Press, Cambridge, 160–206.

Thorpe RS (1975) Quantitative handling of characters useful in snake systematics with particular reference to intraspecific variation in the ringed snake *Natrix natrix*. Biological Journal of the Linnean Society 7: 27–43. https://doi.org/10.1111/j.1095-8312.1975.tb00732.x

Thorpe RS (1983) A review of the numerical methods for recognizing and analyzing racial differentiation. In: Felsenstein J (Ed.) Numerical Taxonomy. NATO ASI Series, Volume 1. Springer, Berlin, Heidelberg: 404–423. https://doi.org/10.1007/978-3-642-69024-2_43

Tshewang S, Letro L (2018) The herpetofauna of Jigme Singye Wangchuck National Park in central Bhutan: Status, distribution and new records. Journal of Threatened Taxa 10: 12489–12498.

Turan C (1999) A note on the examination of morphometric differentiation among fish populations: The Truss System. Turkish Journal of Zoology 23: 259–263.

Uetz P, Freed P, Aguilar R, Reyes F, Hošek J (2023) The Reptile Database. Available from URL: http://www.reptile-database.org [accessed 11 June 2023].

Vindum JV, Win H, Thin T, Lwin KS, Shein AK, Tun H (2003) A new species of *Calotes* (Squamata: Agamidae) from the Indo-Burman range of western Myanmar. Proceedings of the California Academy of Sciences 54: 1–16.

Wagner P, Ihlow F, Hartmann T, Flecks M, Schmitz A, Böhme W (2021) Integrative approach to resolve the *Calotes mystaceus* Duméril and Bibron, 1837 species complex (Squamata: Agamidae) Bonn zoological Bulletin 70: 141–171. https://doi.org/10.20363/BZB-2021.70.1.141

Wang K, Lyu ZT, Wang J, Qi S, Che J (2022) The updated checklist and zoogeographic division of the reptilian fauna of Yunnan Province, China. Biodiversity Science 30: 213–226 [in Chinese]. https://doi.org/10.17520/biods.2021326

Wang K, Jiang K, Deepak V, Abhijit D, Hou M, Che J, Siler CD (2018) On the occurrences of *Japalura kumaonensis* and *Japalura tricarinata* (Reptilia: Sauria: Draconinae) in China. Herpetologica 74: 181–190. https://doi.org/10.1655/Herpetologica-D-17-00018.1

Wang K, Che J, Lin S, Deepak V, Aniruddha DR, Jiang K, Jin J, Chen H, Siler CD (2019) Multilocus phylogeny and revised classification for mountain dragons of the genus *Japalura* s. l. (Reptilia: Agamidae: Draconinae) from Asia. Zoological Journal of the Linnean Society 185: 246–267. https://doi.org/10.1093/zoolinnean/zly034

Wang K; Ren JL, Chen HM, Lyu ZT, Guo XG, Jiang K, Chen JM, Li JT, Guo P, Wang Y, Che J (2020) The updated checklists of amphibians and reptiles of China. Biodiversity Science 28: 189–218 [in Chinese]. https://doi.org/10.17520/biods.2019238

Yang DT, Rao DQ (2008) Amphibia and Reptilia of Yunnan. Yunnan Science and Technology Press, Kunming, 411 pp. [in Chinese].

Yingjiang.gov.cn: Wildlife poaching confiscated in Yingjiang. Available from URL: http://www.yingjiang.gov.cn/jinriyingjiang/yingjiangxinwen/content-15-9480-1.html [accessed 11 June 2023].

Zhao EM, Li SQ (1984) A new species of *Calotes* (Lacertilia: Agamidae) from Xizang (Tibet) Acta Herpetologica Sinica 3: 77–78 [in Chinese].

Zhao EM, Adler K (1993) Herpetology of China. Society for the Study of Amphibians and Reptiles, Oxford, OH, 522 pp.

Zhao EM, Yang DT (1997) Amphibians and Reptiles of Hengduan Mountains. Science Press, Beijing, 303 pp. [in Chinese].

Zhao EM, Zhao KT, Zhou KY et al. (1999) Fauna Sinica Reptilia: Squamata: Lacertilia. Science Press, Beijing, 394 pp.

Zug GR, Brown HH, Schulte JA, Vindum JV (2006) Systematics of the garden lizards, *Calotes versicolor* group (Reptilia, Squamata, Agamidae), in Myanmar: Central dry zone populations. Proceedings of the California Academy of Sciences 57: 35–68.

Supplementary Material 1

Appendices I–VII

Authors: Wang K, Deepak V, Das A, Grismer LL, Liu S, Che J (2024)
Data type: .xlsx
Explanation notes: This appendix file contains Appendices I–VII, which include voucher info. for specimens examined, GenBank info. for phylogenetic analyses, raw morphological data for *Calotes jerdoni* complex examined, raw morphological data for type series of the new species described, and detailed statistics for the morphological analyses.

Link: https://doi.org/vz.74.e109088.suppl1